Lithos 316–317 (2018) 304–322

Contents lists available at ScienceDirect

Lithos

journal homepage: www.elsevier.com/locate/lithos

Sub-lithospheric origin of Na-alkaline and calc-alkaline magmas in a post-collisional tectonic regime: Sr-Nd-Pb isotopes in recent monogenetic volcanism of Cappadocia, Central Turkey

Paolo Di Giuseppe [a,b], Samuele Agostini [a,**], Piero Manetti [a,c], Mehmet Yilmaz Savaşçın [d], Sandro Conticelli [c,e,*]

[a] Istituto di Geoscienze e Georisorse, Consiglio Nazionale delle Ricerche, Via Moruzzi, 1, I-56124 Pisa, Italy
[b] Dipartimento di Scienze della Terra, Università degli Studi di Pisa, Via Santa Maria, 53, I-56126 Pisa, Italy
[c] Dipartimento di Scienze della Terra, Università degli Studi di Firenze, Via Giorgio La Pira, 4, I-50121 Firenze, Italy
[d] Jeoloji Mühendisliği, Munzur Üniversitesi, Bölümü 62000, Merkez, Tunceli, Turkey
[e] Istituto di Geologia Ambientale e Geoingegneria, Consiglio Nazionale delle Ricerche, Via Salaria km 29,300, I-00015 Monterotondo, Italy

ARTICLE INFO

Article history:
Received 16 April 2018
Accepted 16 July 2018
Available online 20 July 2018

Keywords:
Central Anatolia
Cappadocia
Pleistocene volcanic rocks
K-Ar ages
Geochemistry
Isotope geochemistry
Geodynamics

ABSTRACT

Intense Cenozoic magmatism accompanied the convergence and collision of the Eurasian, African and Arabian plates. In the Cappadocia Region of Central Anatolia, widespread and abundant volcanism developed from the late Miocene to the Quaternary. Calc-alkaline pyroclastic products and lava erupted diffusely during the late Miocene and Pliocene. Both calc-alkaline and Na-alkaline volcanic rocks were emplaced in close spatial and temporal proximity during the Plio-Pleistocene. Here we focus on the Plio-Pleistocene monogenetic activity, which produced two types of rocks: calc-alkaline volcanic rocks ranging in composition from basalts to rhyolites and occurring around the Acıgöl caldera, the Göllü Dağ dome and the Hasan Dağ and Erciyes Dağ composite volcanoes; Na-alkaline volcanic rocks ranging from alkali basalts to mugearites and cropping out in monogenetic centres in Karapınar, along the WSW flank of Hasan Dağ, in Acıgöl and near the Kızılırmak River, northwest of Nevşehir.
The coeval occurrence of calc-alkaline and Na-alkaline volcanism observed here is in striking contrast with activity in the surrounding Western and Eastern Anatolia regions, where the calc-alkaline volcanic rocks are distinctly older than the Na-alkaline ones. The Sr and Nd isotopic compositions of the mantle sources of both rock types show a narrow, overlapping range of values ($^{87}Sr/^{86}Sr$~0.70395–0.70474 and $^{143}Nd/^{144}Nd$~0.51268–0.51281 for the calc-alkaline products, 0.70334–0.70524 and 0.51268–0.51293 for the Na-alkaline ones). In addition, most of the Na-alkaline products, like the calc-alkaline rocks, show an arc-type distribution of incompatible trace elements, with marked enrichments in LILE (Large-Ion Lithophile Elements) and negative HFSE (High Field Strength Elements) anomalies. True intraplate magmas are absent in Cappadocia, where the genesis of Na-alkaline basalts is ascribed to mixing between different percentages of within-plate (OIB) and calc-alkaline magmas. Modelling reveals that the addition of 13% and 30% OIB-type melt to a calc-alkaline magma is enough to change a SiO_2-oversaturated magma into an *ol-hy*-normative and *ne*-normative one, respectively, whereas the addition of 15% calc-alkaline magma to an OIB-type magma results in a negative Nb—Ta anomaly in the primitive mantle-normalized spider diagrams.
The various types of products of recent volcanism in Cappadocia reflect the complex tectonic setting of the Central Anatolian Block: characterised by strike-slip tectonics and local extensional pull-apart basins, different magma types formed contemporaneously through decompression melting at different depths.
In this scenario, the calc-alkaline magmas derived from partial melting of a mantle wedge modified by a subduction component, whereas the within-plate (OIB) magmas derived from a deeper, unmodified sub-slab mantle source. Mixing between calc-alkaline and within-plate magmas during their rise to the surface produced the Na-alkaline Cappadocia basalts. The very low rate of extension allowed within-plate magmas (OIB) to reach the surface after having interacted with the overlying calc-alkaline magmas in the late stages of Cappadocia volcanism.

* Correspondence to: Sandro Conticelli, DST-Università di Firenze, Via Giorgio La PIra, 4, I-50121 Firenze, Italy.
** Correspondence to: Samuele Agostini, IGG-CNR, Via Moruzzi, 1, Pisa I-56124, Italy.
E-mail addresses: s.agostini@igg.cnr (S. Agostini), sandro.conticelli@unifi.it (S. Conticelli).

https://doi.org/10.1016/j.lithos.2018.07.018

1. Introduction

Convergent destructive plate margins are sites of intense volcanism that sometimes produce igneous rocks with contrasting petrological characteristics due to interaction among different geochemical reservoirs recycled within the mantle wedge (e.g., Arculus and Powell, 1986; Avanzinelli et al., 2012; Elliott et al., 1997; Hawkesworth et al., 1991, 1993; Pearce, 1983; Plank, 2005; Plank and Langmuir, 1998). When destructive plate margins involve the continental lithosphere, the dynamics of the converging plates may produce tears and incisions that channel deep reservoirs into the mantle wedge, thereby increasing the complexity of magma genesis and evolution in the post-collisional setting (e.g., Avanzinelli et al., 2009; Bonin, 2004; Gasperini et al., 2002; Smith et al., 2001; Turner and Hawkesworth, 1998). The Mediterranean region, with its complex geodynamic setting and wide range of magma types occurring in close spatial and temporal proximity, is an ideal site for studying multi-stage magma genesis during the tectonic evolution of collision zones (e.g., Agostini et al., 2007, 2010a; Conticelli et al., 2009, 2011, 2013, 2015; Duggen et al., 2005; Faccenna et al., 2006; Lustrino et al., 2011; Lustrino and Wilson, 2007; Prelević et al., 2012; Serri et al., 2001).

In the Mediterranean region, Anatolian Neogene volcanism has some of the best examples for in-depth investigation of the transition from subduction-related (i.e., calc-alkaline, high-K calc-alkaline, shoshonitic, and potassic alkaline rocks) to within-plate (i.e., Na-alkaline) volcanism. In the Eastern Mediterranean, the collision of the African and Arabian plates with Eurasia led to the formation of magmas with an arc signature that shifted, in time and space, to post-collisional products and Na-alkaline within-plate magmatism, as seen from the western margin of Anatolia to its eastern end, from the Biga-Izmir region in the Aegean sector to the Kula area, Cappadocia and the Malatya region in Central Anatolia, Elazığ-Karlıova and the eastern part of the Van region (e.g., Agostini et al., 2007, 2010a, 2010b, 2016, 2018; Aldanmaz et al., 2000; Di Giuseppe et al., 2017; Doglioni et al., 2002). In particular, the Cappadocia Region of Central Anatolia was the centre of abundant monogenetic late Pliocene-Holocene volcanism. Here the emplacement of extensive post-collisional subduction-related medium- to high-K calc-alkaline lavas and ignimbrites was followed by younger bimodal volcanism (e.g. Aydin et al., 2014). In contrast to the volcanic provinces in Western and Eastern Anatolia, the transition from subduction-related volcanism to within-plate magmatism in Cappadocia is unclear in terms of timing and evolution, with complete overlapping of the two (e.g., Dogan-Kulachı et al., 2018; Gençalioğlu-Kuşcu and Geneli, 2010).

This paper reports new and original geological, petrological, geochemical and isotopic data on fifty-one rock samples representative of monogenetic volcanic activity in Karapınar, the Acıgöl-Nevşehir magmatic complex, Kızılırmak and around the two main strato-volcanoes in the Cappadocia Region (i.e., Hasan Dağ and Erciyes Dağ). Detailed Sr-Nd-Pb isotope studies on these rocks were undertaken to better understand the geodynamic evolution of Central Anatolia and the involvement of different mantle sources, namely the relationship between subduction-related and within-plate magmatism in the Eastern Mediterranean region.

2. Geological background

2.1. Geodynamic context

Anatolia is part of the Cenozoic Alpine-Himalayan orogenic belt, which formed through the collision of different continental blocks derived from the northern part of Gondwana (e.g., the Sakarya and Kirşehir microplates).

Three different domains can be identified from north to south: the Pontides, the Anatolian Block, and the Taurides (Fig. 1). The main tectonic features of Anatolia formed due to the closure of the multi-branched Tethyan Ocean during the Mesozoic and Cenozoic (Şengör and Yılmaz, 1981). After the closure of the Palaeotethys, the Neotethys

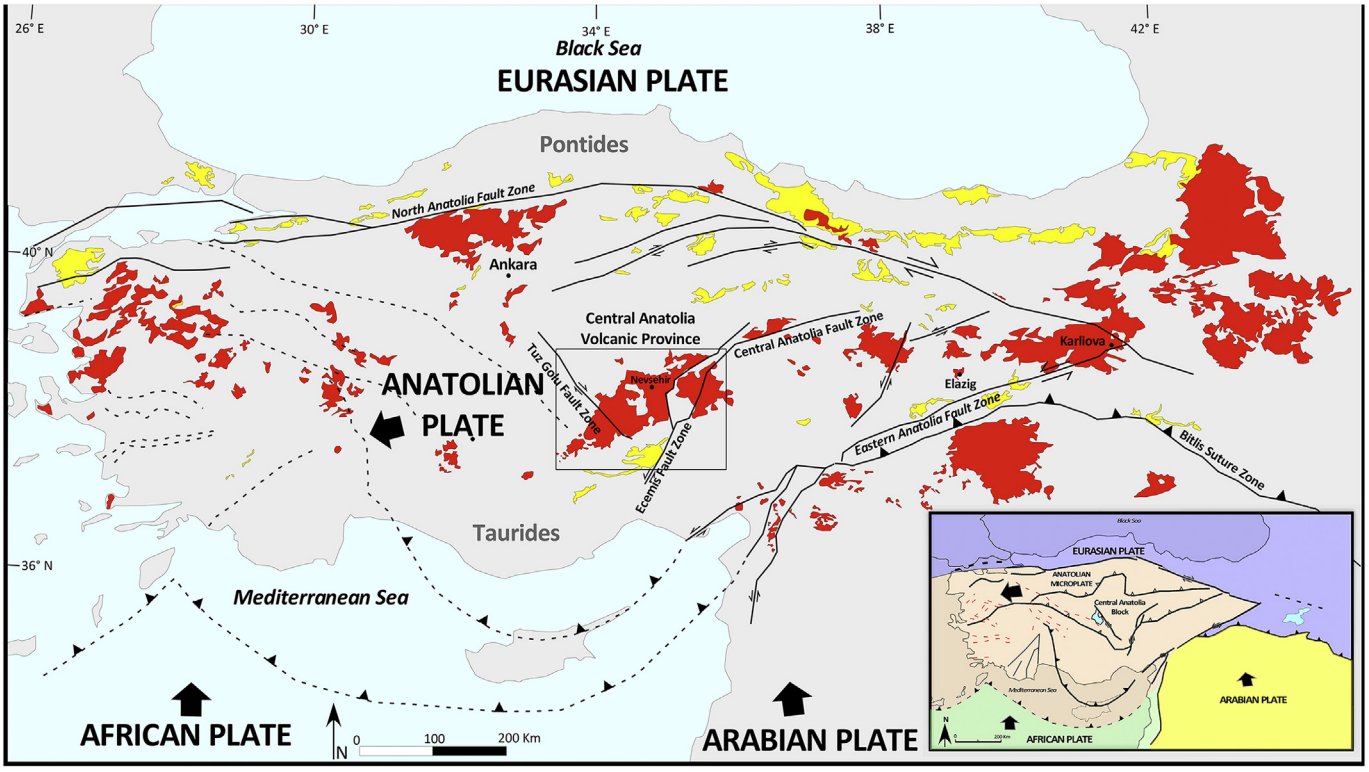

Fig. 1. Sketch map of the Anatolia microplate and adjoining regions showing the main structural features and volcanic activity: Palaeogene volcanism in yellow, Neogene magmatism in red (modified after Uslular et al., 2015). The inset reports the tectonic setting of the region and shows the interaction between the Arabian, African and Eurasian plates. Big arrows represent the motion of the tectonic plates relative to Eurasia. The rectangle delimits the study area (see Fig. 2).

Ocean started to subduct along the Eurasian margin as a consequence of the northward convergence between Arabia-Africa and the Eurasian Plate. During the Oligocene, the Arabian and African plates became independent due to the opening of the Gulf of Aden-Red Sea and the Suez Gulf (Le Pichon and Gaulier, 1988; McKenzie et al., 1970; Shaw et al., 2003). To the east, the Arabia-Eurasia convergence culminated with a continent-continent collision along the Bitlis-Zagros suture zone (Fig. 1) in the middle Miocene (Bozkurt, 2001; Dewey et al., 1986; Faccenna et al., 2006; Şengör and Yılmaz, 1981); to the west, beginning at least in the early Miocene, the African Plate started to subduct beneath Eurasia along the Aegean and Cyprus trenches (e.g., Agostini et al., 2010a). These dynamics were responsible for deformation and the westward drift of the Anatolian block (Fig. 1), which led to a) shortening and thickening of the crust in Eastern Anatolia (Şengör et al., 2003), b) back-arc extension in Western Anatolia (e.g. Agostini et al., 2010a), and c) activation of the *E*-W trending North Anatolian Fault (middle Miocene, Şengör et al., 2005) and the SSW-NNE trending East Anatolian Fault (late Miocene, Bozkurt, 2001; Karaoğlu et al., 2017; Taymaz et al., 1991). The North Anatolian Fault and the East Anatolian Fault merge to form a triple junction among the Eurasian, Arabian, and Anatolian continental plates (i.e., Karlıova Triple Junction, Fig. 1). Intense magmatic activity accompanied these tectonic events.

In particular, Central Anatolia was characterised by the late Eocene-middle Miocene development of compressive faults that were subsequently reactivated as transcurrent faults with a normal component (e.g. the Ecemiş and Tuz Gölü faults) during the late Miocene-early Pliocene (Fig. 1; Dirik and Göncüoğlu, 1996; Göncüoglu and Toprak, 1992; Jaffey et al., 2004; Özsayin et al., 2013), resulting in basin subsidence and favouring the widespread middle Miocene to Recent post-collision volcanism (e.g., Notsu et al., 1995; Pasquaré et al., 1988 and references therein).

2.2. The Central Anatolia Volcanic Province

The Central Anatolia Volcanic Province (Toprak and Göncüoğlu, 1993; Fig. 1) is located within the Central Anatolian Crystalline Complex north of the Tauride Belt (Şengör and Yılmaz, 1981); it is a Neogene-Quaternary volcanic field forming a narrow belt that extends for 300 km in a NNE-SSW direction and has a variable width of 25 to 50 km (Fig. 2).

The volcanic centres and their associated volcanic rocks are roughly aligned along the Central Anatolian Fault Zone, which in the Cappadocia area is represented by the Ecemiş Fault (Fig. 2), a NE-SW left-lateral strike-slip fault intersecting the Cretaceous metamorphic basement of the Niğde Massif and Kirşehir Massifs (Dirik and Göncüoğlu, 1996; Piper et al., 2013).

The central-western sector is bounded by two main transcurrent faults: the Tuz Gölü Fault, to the southwest, and the Salanda Fault, to

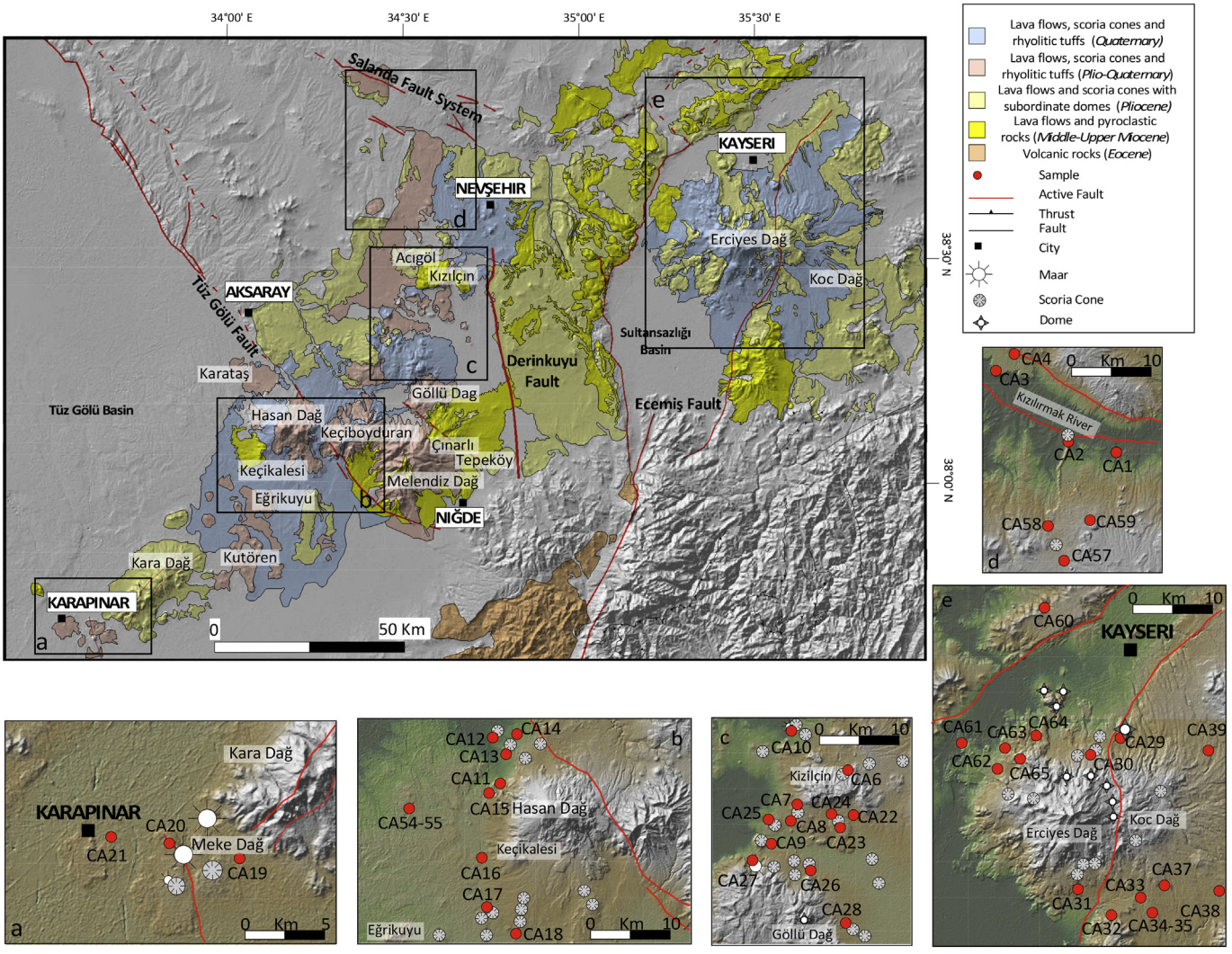

Fig. 2. Simplified tectonic and volcanological map of the Central Anatolia Volcanic Province. The region is subdivided into five different clusters here delimited by rectangles; a) Karapınar; b) Hasan Dağ; c) Acıgöl-Nevşehir; d) Kızılırmak; e) Erciyes Dağ.

the north (Fig. 2). The westernmost portion of the Tuz Gölü Fault System consists of parallel to subparallel, normal and oblique right-lateral strike-slip faults displaying a step-like half-graben and horst-graben pattern (Dhont et al., 1998; Dirik et al., 1999; Dirik and Göncüoğlu, 1996). The Salanda dextral strike-slip fault system trends WNW-ESE and is characterised by numerous short to long, closely-spaced structural fault segments and fault sets, such as the Tuzköy and the Avanos faults (Dirik et al., 1999; Koçyiğit and Doğan, 2016).

Most of the tectonic structures developed within the Mio-Pliocene volcanoclastic rocks and were subsequently covered by volcanic products. They show ENE-WSW to NE-SW strike and are characterised by a normal component. The major volcanic centres are also roughly aligned along the same directions (Toprak and Göncüoğlu, 1993). A complex system of volcano-tectonic depressions developed within this framework, starting from the Middle-late Miocene (e.g., Innocenti et al., 1975; Le Pennec et al., 1994; Pasquaré et al., 1988; Toprak, 1998).

2.3. The volcanic sequence

The Central Anatolia Volcanic Province is characterised by late Neogene-Quaternary polygenetic composite to monogenetic volcanoes. The main volcanological features include scoria cones, tuff cones and maars, mafic to felsic lava flows, domes and extensive ignimbrite sheets, which form a large volcanic plateau covering ca. 40,000 km^2 (Fig. 2). Among the composite volcanoes, the Hasan Dağ, Erciyes Dağ, Melendiz Dağ and Keçiboyduran are the most important edifices, whereas ignimbrites are thought to have erupted from the Melendiz, Ciftlik, Acıgöl and Derinkuyu caldera complexes (Le Pennec et al., 1994, 2005; Pasquaré et al., 1988; Temel et al., 1998), southwest of Nevşehir, and from the Keçikalesi and Kizilçin volcanoes (Aydar and Gourgaud, 1998; Toprak, 1998), which are presently covered by the products of the younger Hasan Dağ stratovolcano. Monogenetic volcanoes dot the entire volcanic province, with domes such as the Gollü Dağ and maars such the Acıgöl, as well as several hundred scoria cones (Fig. 2).

The oldest volcanic rocks in the Central Anatolia Volcanic Province are the basaltic andesite lavas of Keçikalesi (13.7–12.4 Ma, Besang et al., 1977) and Kizilçin volcanoes (13.7–6.5 Ma, Batum, 1978), followed closely by several large ignimbrites sheets usually grouped in the Ürgüp Formation (Pasquaré, 1968), with an age of 11.2–2.7 Ma (Fig. 2, Supplementary Table 1; e.g., Lepetit et al., 2014 and references therein) and mainly characterised by high-k dacitic to rhyolitic compositions (Temel et al., 1998).

Large composite volcanoes, such as Kara Dağ, Hasan Dağ, Keçiboyduran, Melendiz Dağ, Tepeköy, Çınarlı, and Erciyes Dağ (Fig. 2), began to form in the late Miocene and mainly during the Plio-Quaternary (7.21 Ma to Recent, see Supplementary Table 1 for references). The products of these volcanoes are mainly lava flows interbedded with pyroclastic rocks having a high-K calc-alkaline petrological affinity, ranging from basaltic andesite to dacite (e.g., Alici Şen et al., 2004; Aydar and Gourgaud, 1998; Aydin, 2008; Deniel et al., 1998; Gençalioğlu-Kuşcu and Geneli, 2010; Kürkçüoğlu et al., 1998, 2001; Notsu et al., 1995).

2.4. The most recent volcanic activity in Cappadocia

The most recent volcanic activity in Cappadocia occurred mainly in the peripheral areas of the major composite volcanic apparata of the region (e.g., Karapınar, Eğrikuyu, South Hasan Dağ, Karataş, Acıgöl, Kutören volcanic fields and the areas peripheral to the Erciyes Dağ, Fig. 2). This monogenetic activity was in some cases coeval with that of the composite volcanoes, and frequently continued until the Recent (e.g., from 2.57 to 0.002 Ma; e.g., Aydar et al., 2013; Batum, 1978; Bigazzi et al., 1993; Dogan-Kulachı et al., 2018; Reid et al., 2017).

The monogenetic volcanic fields consist of mafic volcanic rocks with a bimodal petrochemical character ranging from SiO_2-oversaturated calc-alkaline samples to SiO_2-undersaturated Na-alkaline ones (e.g, Alici Şen et al., 2004; Aydin, 2008; Dogan-Kulachı et al., 2018; Gençalioğlu-Kuşcu and Geneli, 2010; Notsu et al., 1995).

The study area was divided into five volcanic clusters in order to better define the area of provenance of the most recent magmatic products, which are consistently and persistently related to monogenetic volcanic centres spread out along the SW-NE volcanic alignment observed for the older Cappadocia volcanism (Fig. 2). However, control by local, rather than regional, tectonics may in some cases give rise to different small-scale distribution patterns.

The southwesternmost volcanic cluster, located near the town of Karapınar (Fig. 2), consists of several cinder cones, two lava fields and four maars (Keller, 1974) aligned in a SW-NE direction parallel to the main regional trend of Cappadocia volcanism.

The second volcanic cluster is some ten kilometres northeast of Karadağ and west of the Hasan Dağ composite volcano. The cinder cones of this recent monogenetic activity are arranged radially around the Hasan Dağ twin volcano (Fig. 2b). Lava flows from cinder cones have basaltic compositions and were active during the Neo Hasan Dağ stage (Notsu et al., 1995).

In the central area of the Cappadocia volcanic region lies the Acıgöl-Nevşehir volcanic cluster, with recent lava domes, tuff rings, maars, scoria cones and lava flows randomly distributed between the Göllü Dağ dome and the Kizilçin composite volcano (Fig.2c). Recent volcanism is characterised by basaltic-rhyolitic bimodal activity (Aydin, 2008; Druitt et al., 1995; Toprak, 1998).

The fourth volcanic cluster is found near the Kızılırmak River, in the northernmost sector of central Cappadocia, with the centres aligned and within the NNW-SSE parallel to the Salanda and Tepeköy fault systems (Fig. 2d). Rare cinder cones and basaltic lava flows of differing age (2–0.1 Ma) and thickness (Doğan, 2011) were emplaced mainly on the ignimbrite of the Ürgüp Formation, on the older rocks of the Paleozoic basement of the Kirşehir Massif and on the middle Miocene sedimentary Tüzköy Formation (Koçyiğit and Doğan, 2016).

The fifth volcanic cluster lies around the Erciyes Dağ composite volcano. Erciyes Dağ represents the most prominent relief of Central Anatolia and is located within the Sultansazlığı pull-apart basin. Recent monogenetic activity (domes and cinder cones) is distributed along the northwestern and southeastern flanks of the Erciyes Dağ Volcano (Fig. 2e) and has produced volcanic products with a clear bimodal basalt-rhyolite composition.

3. Material and methods

Previous studies about the late volcanic activity in Cappadocia reported the occurrence of calc-alkaline and Na-alkaline igneous rocks with unknown temporal relationships and correlations (Le Pennec et al., 1994). Recent studies pointed out the contemporaneous emplacement of subduction-related magmas and products with intraplate signatures, with the effect of subduction decreasing from Miocene to the Quaternary time (Dogan-Kulachı, 2016; Doğan-Külachı et al., 2016, 2018). We focus on the Plio-Pleistocene monogenetic volcanic activity to address the issue of the shift from subduction-related to within-plate magmas in the Central Anatolia region. With this in mind we divided the study area into five distinct volcanic clusters: Kızılırmak, Erciyes Dağ, Acıgöl-Nevşehir, Hasan Dağ and Karapınar (Fig. 2).

The studied rocks were mainly collected from lava flows, and to a lesser extent from scoria cones. Geographic details, along with outcrop locality, type of rock, petrography and GPS coordinates are shown in Supplementary Table 2). A total of fifty-one rock samples from Central Anatolia Volcanic Province were analysed to determine the whole-rock chemistry. These were collected from the five clusters described above (Fig. 2): seven (7) from the Kızılırmak area, along the river of the same name, seventeen (17) from the peripheral areas of the Erciyes Dağ composite volcano, thirteen (13) from the Acıgöl-Nevşehir Complex, eleven (11) from the western slope of Hasan Dağ stratovolcano

Table 1
Major and trace elements, and initial radiogenic isotope data of selected samples.

Sample	CA 57	CA 2	CA 1	CA 27	CA 26	CA 28	CA 11	CA 14	CA 16	CA 12	CA 20	CA 21	CA 29	CA 62	CA 32	CA 38
Locality	Kızılırmak			Acıgöl-Nevşehir			Hasan Dağ				Karapınar		Ercyies Dağ			
Rock Type	Alk	Alk	CA	Alk	Alk	CA	Alk	Alk	Alk	Alk	Alk	CA	CA	CA	CA	CA
	Basalt	Mugearite	Bas. And.	Basalt	Basalt	Andesite	Basalt	Basalt	Hawaiite	Hawaiite	Hawaiite	Bas. And.	Basalt	Bas. And.	Bas. And.	Bas. And.
Major elements (wt%)[a]																
SiO_2	48.69	51.37	53.06	48.26	49.44	62.93	49.81	50.57	50.24	51.41	51.08	52.42	51.58	53.05	53.19	55.05
TiO_2	1.38	2.25	1.26	1.54	1.18	0.71	1.18	1.23	1.50	1.45	1.33	1.01	1.43	1.38	1.50	1.70
Al_2O_3	18.04	16.94	16.96	16.66	17.93	15.25	15.81	16.34	16.58	16.91	17.95	16.15	17.62	17.62	17.44	17.58
Fe_2O_3	1.07	3.32	0.92	1.53	1.91	0.52	3.32	2.05	1.91	2.12	3.08	2.46	1.48	2.45	2.47	1.05
FeO	7.22	6.41	6.57	8.15	6.77	4.04	5.37	6.22	6.74	5.94	5.85	5.30	6.92	5.38	6.03	7.34
MnO	0.14	0.17	0.13	0.16	0.14	0.10	0.15	0.14	0.14	0.13	0.14	0.13	0.14	0.13	0.13	0.13
MgO	8.58	4.73	6.89	9.63	7.55	4.02	9.49	8.35	8.60	7.30	5.73	8.64	6.45	5.66	5.05	4.24
CaO	11.02	7.68	8.80	9.25	10.95	5.56	9.76	9.46	8.51	8.63	9.06	8.71	9.36	7.91	8.78	6.81
Na_2O	3.12	4.70	3.70	3.56	3.09	3.94	3.40	3.67	3.79	3.91	4.02	3.41	3.91	4.19	3.97	4.13
K_2O	0.18	1.48	1.18	0.53	0.47	2.63	1.08	1.23	1.24	1.46	1.12	1.19	0.50	1.41	0.89	1.13
P_2O_5	0.15	0.61	0.18	0.27	0.19	0.11	0.34	0.40	0.37	0.40	0.32	0.29	0.23	0.53	0.24	0.45
LOI	0.55	0.67	0.57	0.69	0.60	0.65	0.51	0.37	0.77	0.43	0.46	0.66	0.47	0.53	0.67	0.64
Total	99.59	99.66	99.65	99.54	99.62	99.81	99.71	99.66	99.62	99.66	99.68	99.71	99.62	99.71	99.69	99.61
Trace elements (μg/g)[a]																
Sc	30	21	25	24	36	19	24	23	24	21	17	29	39	22	24	22
V	193	183	160	190	212	91	186	175	185	167	155	170	192	148	177	154
Cr	242	30	163	389	76	136	356	280	285	195	39	321	171	129	42	30
Co	42	28	35	45	38	18	38	36	39	32	22	34	34	27	29	27
Ga	15	20	16	15	16	14	17	17	16	17	13	15	17	18	18	20
Rb	2	28	25	6	8	71	16	23	21	27	17	26	6	26	15	12
Sr	431	542	354	390	500	245	598	590	580	621	446	658	436	636	426	478
Y	23	40	25	25	21	19	25	26	26	25	21	22	27	27	29	31
Zr	118	275	146	154	101	150	145	162	162	164	98	145	157	218	164	205
Nb	3	18	7	8	5	12	15	16	14	17	7	11	6	22	7	13
Cs	0.1	0.5	0.6	0.3	0.3	2.4	0.2	0.6	0.5	0.6	0.4	0.9	0.1	0.9	0.4	0.3
Ba	52	310	245	95	131	487	380	385	291	376	237	409	133	424	214	343
La	5.6	31.8	15.9	11.1	11.7	42.0	29.8	31.2	23.7	28.0	20.0	32.5	10.9	31.9	15.4	23.1
Ce	16.0	68.7	32.8	27.8	26.4	71.0	59.1	62.2	50.0	55.6	39.7	63.0	26.4	67.0	33.4	50.0
Pr	2.30	8.46	4.01	3.60	3.20	6.50	6.92	7.15	6.17	6.60	4.72	6.60	3.40	7.50	4.41	6.00
Nd	11.1	34.8	16.5	15.6	13.6	21.0	26.4	27.4	24.4	25.6	18.8	24.0	15.1	28.9	18.8	25.0
Sm	3.1	7.1	3.7	3.8	3.3	3.5	4.9	5.2	4.8	4.8	3.8	4.3	3.8	5.7	4.6	5.6
Eu	1.24	2.26	1.26	1.36	1.17	0.85	1.48	1.56	1.57	1.49	1.13	1.31	1.39	1.76	1.50	1.88
Gd	3.5	7.0	3.9	4.1	3.5	3.2	4.5	4.9	4.6	4.5	3.5	4.2	4.1	5.5	4.6	5.5
Tb	0.64	1.19	0.67	0.72	0.60	0.52	0.72	0.76	0.75	0.72	0.57	0.64	0.73	0.84	0.79	0.91
Dy	4.0	6.8	4.1	4.5	3.7	3.2	4.2	4.3	4.4	4.3	3.4	3.8	4.6	4.9	4.6	5.5
Ho	0.87	1.40	0.90	0.97	0.79	0.67	0.87	0.92	0.92	0.88	0.76	0.79	0.99	1.01	1.04	1.13
Er	2.5	3.9	2.4	2.8	2.3	2.0	2.5	2.5	2.5	2.5	2.0	2.3	2.8	2.9	2.8	3.2
Tm	0.35	0.58	0.36	0.40	0.33	0.30	0.36	0.36	0.37	0.35	0.30	0.33	0.41	0.41	0.40	0.46
Yb	2.1	3.4	2.3	2.5	2.0	1.9	2.2	2.2	2.2	2.1	1.9	2.1	2.5	2.5	2.6	2.8
Lu	0.33	0.50	0.33	0.37	0.30	0.30	0.32	0.33	0.31	0.32	0.28	0.32	0.38	0.38	0.36	0.43
Hf	2.7	5.5	3.4	3.2	2.4	3.9	3.2	3.6	3.6	3.7	2.3	3.2	3.5	4.6	3.7	4.5
Ta	0.2	1.2	0.5	0.5	0.3	0.9	0.9	1.0	0.9	1.1	0.4	0.6	0.4	1.3	0.5	0.9
Pb	0.6	6.4	5.4	1.5	2.9	14.7	5.4	6.7	4.4	5.7	4.5	9.0	2.5	7.9	3.7	7.3
Th	0.4	5.8	4.1	1.3	2.3	22.8	4.9	4.9	3.8	4.5	4.5	9.6	1.5	4.2	2.2	2.1
U	0.1	1.3	1.0	0.3	0.5	3.2	0.8	1.1	0.9	1.0	0.9	2.0	0.4	1.1	0.7	0.6
Radiogenic isotopes[b]																
$^{87}Sr/^{86}Sr_i$	0.70334	0.70398	0.70399	0.70362	0.70451	0.70405	0.70512	0.70501	0.70441	0.70470	0.70524	0.70553	0.70395	0.70474	0.70457	0.70417
$^{143}Nd/^{144}Nd_i$	0.51293	0.51283	0.51278	0.51289	0.51275	0.51268	0.51268	0.51268	0.51279	0.51271	0.51264	0.51262	0.51281	0.51270	0.51272	0.51275
$^{206}Pb/^{204}Pb_i$	18.851	18.833	18.886	18.785	18.878	18.894	18.900	18.782	18.869	18.882	18.966	18.914	18.931	18.904	18.978	18.782
$^{207}Pb/^{204}Pb_i$	15.592	15.639	15.675	15.617	15.651	15.677	15.668	15.659	15.648	15.667	15.681	15.693	15.644	15.671	15.655	15.660
$^{208}Pb/^{204}Pb_i$	38.659	38.843	38.984	38.751	38.953	39.043	39.003	38.875	38.872	38.982	39.110	39.086	38.937	39.005	38.971	38.874

[a] Complete data set of analysed samples in this study (major and trace elements) along with international reference materials are reported in Supplementary Table 4.
[b] Full data, including measured values and age of correction in Supplementary Table 5.Legend: Alk = Na-alkaline series; CA = Calc-alkaline series; Bas. And. = basaltic andesite.

and three (3) from the Karapınar area, southwest of the Karadağ composite volcano.

In order to complete the geochronological characterisation of the studied rocks, shown in Supplementary Table 1, two samples from the Kızılırmak area were selected for K/Ar age determinations. Dating was performed at the Institute of Nuclear Research of the Hungarian Academy of Sciences. About 500 mg of fresh groundmass samples were spiked with ^{38}Ar for the determination of ^{40}Ar. The mass spectrometer, operating in static mode, was cleaned with conventional getter material prior to gas sample introduction. The HD-B1, GL-O, LP-6 and Asia 1/65 interlaboratory standards were used for calibration. Ages were calculated using the decay constants of Steiger and Jäger (1977). Analytical errors represent one standard deviation. Potassium concentrations were determined by flame photometry, and replicate analyses were reproducible within 2%. K/Ar results are reported in Supplementary Table 3.

Whole-rock major and trace element contents (Table 1 and Supplementary Table 4) were determined at the Dipartimento di Scienze della

Terra of the Università di Pisa by XFR (X-Ray Florescence) and ICP-MS (Inductively Coupled Plasma-Mass Spectrometry), using an ARL 9400 XP^{+}® and a Fisons PQ2 Plus® instrument, respectively. Loss on Ignition was determined by gravimetry. Analytical precisions, assessed by repeated analysis of the in-house standard HE-1 (Mt. Etna hawaiite), was found to be within 2% and 5% RSD, except for Gd (6%), Tm (7%), Pb and Sc (8%). Detection limits for all the elements in the solution were in the 0.002–0.02 ng*ml^{-1} range, except for Ba, Pb and Sr (0.1–0.2) (D'Orazio, 1995).

Sr-Nd-Pb isotope analyses were carried out at the Istituto di Geoscienze e Georisorse – CNR of Pisa (Italy) on sixteen representative samples; results are reported in Table 1 and Supplementary Table 5. Rock powders were dissolved in HF + HNO_3 and, after thorough drying, Sr and REE were purified in HCl solution through ion-exchange chromatography columns. After this process, Nd was separated from other REE using diluted HCl solution passing through an Eichrom® Ln resin. Lead was extracted by matrix after eluting with HBr and HCl. Once separated chromatographically, Sr, Nd and Pb were loaded onto Re filaments and then into the Finnigan Mat 262 thermal ionization mass spectrometer. Sr and Nd isotopic compositions were corrected for mass fractionation using $^{86}Sr/^{88}Sr = 0.1194$ and $^{146}Nd/^{144}Nd = 0.7219$. During the analytical period, the Sr standard NIST SRM 987 and the Nd standard J-Ndi1 yielded average values of $^{87}Sr/^{86}Sr = 0.710239 \pm 0.000017$ (2SD; $n = 43$) and $^{143}Nd/^{144}Nd = 0.512106 \pm 0.000012$ (2SD; $n = 16$), respectively; measured values were adjusted at 0.710250 for $^{87}Sr/^{86}Sr$, whereas no Nd isotope adjustment was required. The Sr and Nd blanks were respectively about 2.3 ng and 1.0, which are negligible for the analysed samples. Lead isotope analyses were performed using a Finnigan MAT 262 multi-collector mass spectrometer operating in static mode. Replicate analyses of Pb isotope ratios are accurate within 0.25‰ (2SD) per mass unit, after applying mass discrimination corrections of 0.15 ± 0.01% per mass unit relative to the NIST SRM 981 reference composition of Todt et al. (1993). Pb blanks were of the order of 0.2–0.4 ng, and no blank correction was made. In addition, Sr, Nd and Pb isotope data were age-corrected (see Supplementary Table 5 for further details).

4. Results

4.1. Ages

Several radiometric age determinations on Cappadocia volcanic rocks are available in the scientific literature (e.g., Aydar et al., 2013; Batum, 1978; Besang et al., 1977; Bigazzi et al., 1993; Dogan-Kulachı et al., 2016, 2018; Ercan et al., 1992; Innocenti et al., 1975; Jaffey et al., 2004; Supplementary Table 1), although very few regard the youngest volcanic rocks (Reid et al., 2017). Because the study focused on the most recent volcanic activity and on the transition from subduction-related to within-plate volcanic rocks, we determined the K—Ar ages of the youngest Na-alkaline basalts (i.e., samples CA 2 and CA 4; Supplementary Table 3). The two analysed samples were collected along the Tepeköy and Salanda fault systems, respectively south and north of the Kızılırmak River. Samples CA 2 and CA 4 yielded ages of 1.74 Ma and 1.94 Ma, respectively (Supplementary Table 3). These data are consistent with those obtained by Doğan (2011) to constrain the stratigraphy and the development of river terraces along the Kızılırmak River. Age of other collected samples were determined according to the literature as reported in Supplementary Table 6.

4.2. Major element chemistry and rock classification

According to the Total Alkali Silica (TAS, Le Maitre, 2002) classification (Fig. 3a), most of the samples are subalkaline, although some of them straddle the alkaline-subalkaline boundary (Irvine and Baragar, 1971). When the feldspathoid silica-saturation index ($\Delta Q = Q\text{-}ne\text{-}lc$; Conticelli et al., 1986) is plotted against the age of rocks, the samples straddling the alkaline-subalkaline boundary fall in the field of silica-undersaturation ($\Delta Q < 0$) (Fig. 3b). These samples are richer in Na_2O than in K_2O (Fig. 3c), suggesting they belong to the Na-alkaline series. In contrast, the silica-saturated samples, characterised by *q* and *hy* in the CIPW norm, belong to the calc-alkaline series (Fig. 3d; Arculus, 2003). In the K_2O vs. SiO_2 diagram for orogenic suites, most of the sub-alkaline samples still fall in the calc-alkaline field, with one sample falling at the lower boundary with the low-K series, and others falling well within the field of the high-K calc-alkaline series (Fig. 3e).

The Na-alkaline rocks show a narrow range of compositions (SiO_2 = 48.2–51.3 and MgO = 9.6–4.7 wt%) spanning from alkaline basalts to hawaiites, with rare mugearites (Fig. 3a). The calc-alkaline rocks instead show a wide compositional range (SiO_2 = 49.4–77.1 and MgO = 8.6–0.1 wt%) representing the complete basalt to rhyolite series. A few samples fall in the fields of basaltic trachyandesites and latites, with one sample falling well within the field of trachytes ($q = 16.3$) in the TAS diagram.

4.3. Petrography

The main petrographic and mineralogical characteristics of the studied samples are reported in Supplementary Table 2. Basalts, hawaiites and basaltic andesites from Karapınar are porphyritic with an olivine + clinopyroxene ± plagioclase phenocryst assemblage, a hypocrystalline groundmass with plagioclase as the most abundant phase and subordinate olivine, clinopyroxene and Ti—Fe oxides.

Lavas collected on the western flank of the Hasan Dağ stratovolcano are partly calc-alkaline and partly Na-alkaline. Their petrography and mineralogy is nevertheless quite similar, with the mineralogical assemblage generally consisting of olivine + clinopyroxene ± plagioclase + Ti—Fe oxides; plagioclase phenocrysts are larger and more abundant in the calc-alkaline rocks, and rare or absent in the Na-alkaline samples. Calc-alkaline andesites are aphyric, with the hypocrystalline groundmass made up of plagioclase, olivine, clinopyroxene and Fe—Ti oxides. Dacites are vitrophyric, with very rare phenocrysts of clinopyroxene and feldspar and pyroxene microliths.

A wide variety of erupted products are found in the Acıgöl-Nevşehir district. Acid products crop out around Acıgöl, where a small caldera is made up of rhyolitic tuff and obsidian lava characterised by a vitrophyric texture with scarce plagioclase + amphibole + quartz crystals. Latitic lava blocks from Göllü Dağ exhibit a porphyritic texture in which plagioclase, amphibole, biotite and rare quartz and clinopyroxene phenocrysts are set in a groundmass consisting of glass and feldspar microliths. Several lava flows, emplaced north of Acıgöl Caldera and between the Erdas Dağ and Göllü Dağ dome complexes, have a calc-alkaline affinity and composition ranging from basaltic andesite, andesite to trachyandesite. They have a porphyritic texture with phenocrysts of plagioclase, clinopyroxene and olivine; plagioclase is also the most abundant phase in the hypocrystalline groundmass, along with clinopyroxene, alkali feldspars and Fe—Ti oxides. In many cases, plagioclase shows partially resorbed sieve and poikilitic textures. In the same region, the Na-alkaline rocks, ranging from alkaline basalts to mugearites, have porphyritic textures in which phenocrysts of plagioclase, olivine and clinopyroxene are set in a hypocrystalline groundmass composed of the same mineral assemblage plus opaque oxides.

Samples from Kızılırmak are either mildly alkaline or calc-alkaline in composition. The alkaline rocks range from alkali basalts to mugearites, whereas calc-alkaline rocks range in composition from basalts to andesites. Their petrography is very similar: all samples are porphyritic with a hypocrystalline groundmass, and their modal mineralogy is dominated by plagioclase, minor amounts of olivine, clinopyroxene and Fe—Ti oxides set in a fine-grained matrix containing intersertal glass.

Samples from monogenetic cones around the Erciyes Dağ composite volcano rocks define a calc-alkaline suite ranging from basaltic andesites to dacites, whereas the most evolved sample (e.g., CA 39) plots in the trachytic field. Dacite and trachyte samples are characterised by a

porphyritic texture with plagioclase, opacitic amphibole, clino- and orthopyroxene, Ti-magnetite, and a hypohyaline groundmass with a feldspar and quartz microcryst assemblage. Andesites and basaltic andesites also show a generally porphyritic texture with a hypocrystalline groundmass: the phenocryst assemblage consists of plagioclase, olivine and minor clinopyroxene in a groundmass containing the same assemblage plus Fe—Ti oxides. Glomeroporphyritic clusters of phenocrysts, including plagioclase and femic phases, are common in these lavas, and plagioclase phenocrysts frequently show sieve textures and oscillatory zoning.

4.4. Major and trace element chemical variations

The Harker diagrams show consistent liquid lines of descent for all major elements but alkalis, although Na-alkaline rocks show trends that differ from those of calc-alkaline samples (Fig. 4, Supplementary Figs. 1–2). All the calc-alkaline rocks show well-defined negative trends for most major elements (e.g., TiO_2, FeO, MgO, MnO, CaO and P_2O_5), a slightly downward convex trend for Al_2O_3, a scattered roughly positive trend for Na_2O, and a focused positive correlation for K_2O. In contrast, Na-alkaline samples show a narrow SiO_2 range, with clear positive trends for Na_2O, K_2O and P_2O_5, scattered trends for TiO_2 and Al_2O_3, and negative correlations with silica for Fe_2O_3, CaO, MgO and MnO (Fig. 4, Supplementary Figs. 1–2).

Selected trace element contents are plotted against silica and $^{87}Sr/^{86}Sr$ in the left and right columns, respectively, of Fig. 4. Although the most primitive samples were selected for trace element determination, large variations in both HFS and LIL element contents are observed at almost constant SiO_2, with a clear overlap between calc-alkaline and Na-alkaline samples. The overlap between the two groups of rocks (i.e., calc-alkaline and Na-alkaline) is confirmed by primitive mantle (PM)- and chondrite-normalized multi-element patterns (Fig. 5). As a whole, the calc-alkaline rocks of the Central Anatolia Volcanic Province are characterised by marked LILE/HFSE enrichments, with all the samples showing pronounced Nb, Ta and Ti troughs and positive K and Pb spikes (Fig. 5a) typical of subduction-related magmas (Hofmann, 1997). REE chondrite-normalized diagrams display fractionated patterns for light and medium REE, and constant heavy REE (Fig. 5a, inset). Compared to normalized patterns for calc-alkaline rocks, Na-alkaline patterns show higher positive Th and U spikes and similar Rb and Ba contents (Fig. 5b). Interestingly, the Na-alkaline rocks have quite different characteristics with respect to typical OIB-HiMu (Sun and McDonough, 1989; Fig. 5b) and to the Na-alkaline basalts cropping out in both Western (e.g. Kula, Innocenti et al., 2005) and Eastern Anatolia (e.g., Elazığ region, Di Giuseppe et al., 2017), which have typical normalized within-plate (OIB-like) trace element patterns (Fig. 5c). The Cappadocia Na-alkaline rocks have variable but negative Nb, Ta, P and Ti anomalies, although in some cases they are fairly similar to those observed for calc-alkaline samples (Fig. 5b). The REE patterns of these rocks closely resemble those observed for the calc-alkaline samples (Fig. 5b, inset). Two rocks belonging to this group show rather different patterns for most incompatible elements: CA 11 and CA 57 have less fractionated patterns, with a small negative Nb—Ta anomaly. In particular, CA 57 has a slight alkaline affinity and is rather close to tholeiitic magmas (e.g. very low K, P and LILE values), with a trace element pattern closely resembling that of *E*-MORBs.

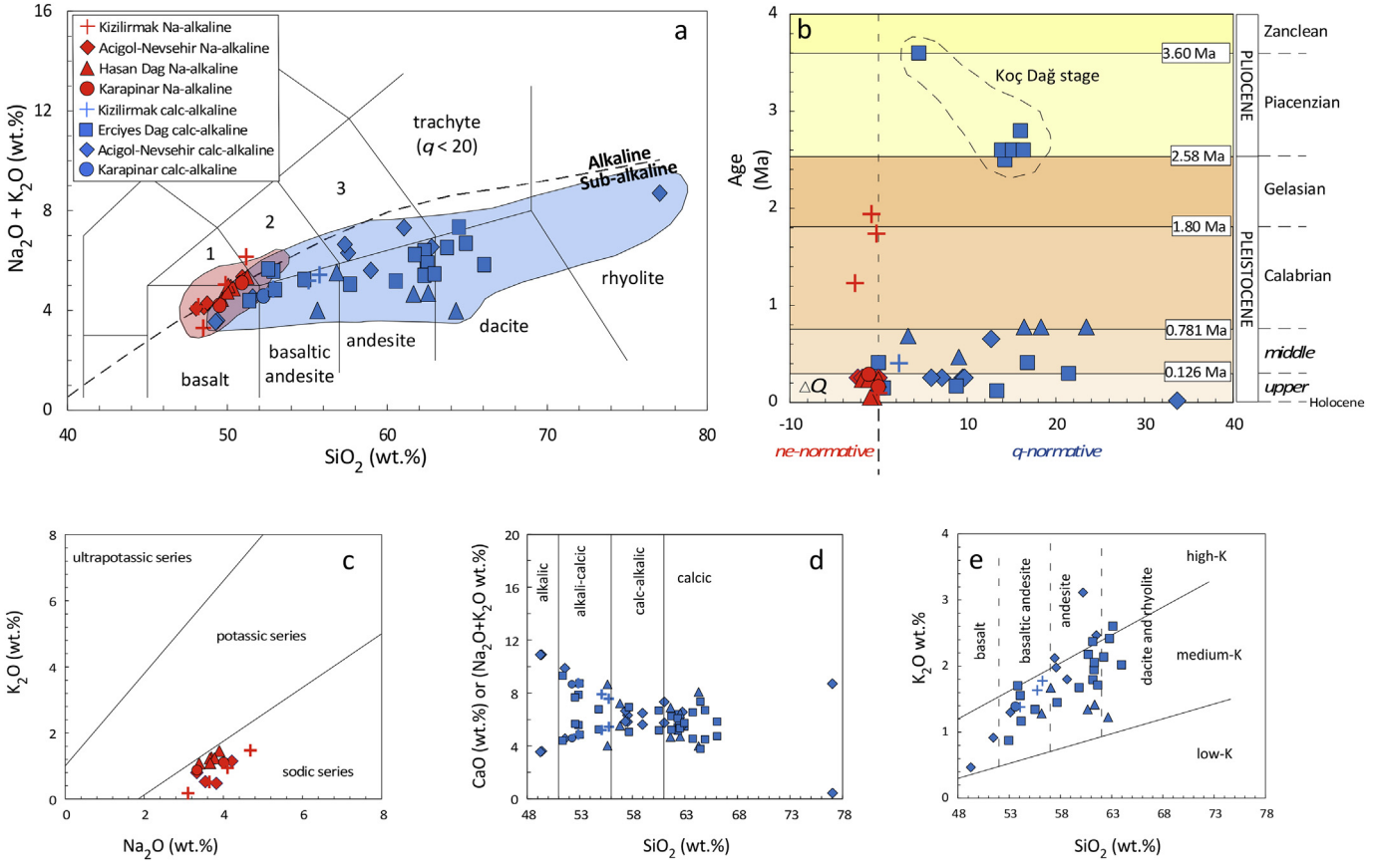

Fig. 3. Classification diagrams for the studied rocks: a) TAS classification diagram (Le Maitre, 2002). Dashed line indicates the boundary between alkaline and sub-alkaline fields according to Irvine and Baragar (1971). Numbered fields represent trachybasaltic (1), andesitic trachybasalt (2) and trachyandesitic (3) fields. According to the TAS classification, rocks with Na_2O-2 > K_2O fields are classified as hawaiites, mugearites or benmoreites; rocks with Na_2O-2 < K_2O are classified as K-trachybasalts, shoshonites or latites. The light red and light blue areas represent the Na-alkaline and calc-alkaline rocks in the Central Anatolia Volcanic Province; b) Age vs. ΔQ diagram (see the text for reference). The vertical dashed line represents the separation between *ne-normative* rocks, on the left, and *q-normative* samples, on the right; c) K_2O vs. Na_2O classification diagram (after Middlemost, 1975); d) CaO or (Na_2O + K_2O) vs. SiO_2 classification diagram (after Arculus, 2003) e) K_2O vs. SiO_2 classification diagram; fields after Le Maitre (2002).

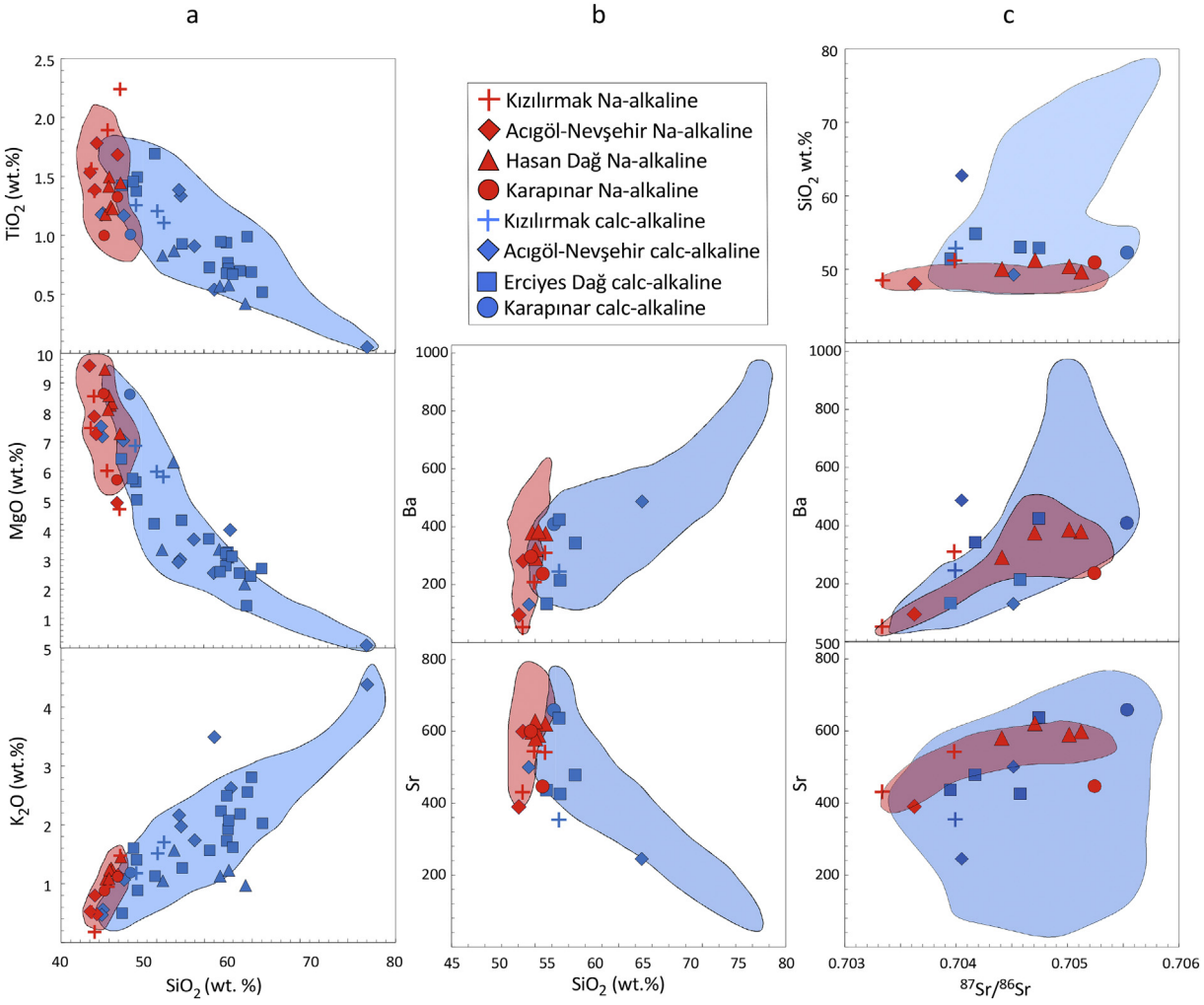

Fig. 4. a) Selected major elements vs. SiO_2 (recalculated on a LOI-free basis) diagrams; b) SiO_2 vs. selected trace elements (Ba, Cr, Sr and Nb); c) $^{87}Sr/^{86}Sr$ vs. selected major and trace elements (SiO_2, Ba, Cr, Sr, Nb). Light red and light blue areas as in Fig. 3.

4.5. Sr, Nd and Pb isotopes

Sixteen representative samples were analysed for Sr-Nd-Pb radiogenic isotopes (Table 1 and Supplementary Table 5; Fig. 6). Selected samples show a relatively large $^{87}Sr/^{86}Sr$ for mafic samples, and a narrow range of SiO_2 and other major element contents (Fig. 4, Supplementary Figs. 1–2); nevertheless, these correlate well, with no distinction between Na-alkaline and calc-alkaline, with trace element variations, both HFSE and LILE (e.g. Ba, Sr, Nb). The same holds true when initial $^{143}Nd/^{144}Nd$ values are plotted against $^{87}Sr/^{86}Sr$ (Fig. 6a), with a negative trend falling on the mantle array and overlapping with that of Eastern Anatolia volcanism. The Sr and Nd isotopic compositions of Cappadocia calc-alkaline rocks differ from those of Western Anatolia calc-alkaline rocks (Fig. 6a), suggesting an isotopically different mantle source. Only two Na-alkali basalt samples (namely CA 57, from Kızılırmak, and CA 27, from Acıgöl-Nevşehir) are characterised by lower Sr and higher Nd isotope ratios (0.70334–0.70362 and 0.51293–0.51289, respectively), both plotting in the field of FoZo (Focal Zone, Fig. 6a) and overlapping with the values of the Na-alkaline rocks of Western and Eastern Anatolia.

The Pb isotope ratios of the studied rocks range from 18.78 to 18.98 for $^{206}Pb/^{204}Pb$, from 15.59 to 15.69 for $^{207}Pb/^{204}Pb$ and from 38.66 to 39.11 for $^{208}Pb/^{204}Pb$ (Fig. 6b). In the $^{206}Pb/^{204}Pb$ vs $^{207}Pb/^{204}Pb$ diagram all the lavas cluster in a small area above the Northern Hemisphere Reference Line (Hart, 1984) and mostly to the left of the field of the EMII end-member. As a whole, the Pb isotopic values of Cappadocia lavas, especially of the Kızılırmak and Acıgöl-Nevşehir rocks showing the lowest values, are similar to those of rocks from Western and Eastern Anatolia. The calc-alkaline rocks show scatter and an almost flat compositional trend for $^{207}Pb/^{204}Pb$ vs. $^{206}Pb/^{204}Pb$ and $^{208}Pb/^{204}Pb$ vs. $^{206}Pb/^{204}Pb$, whereas alkaline rocks define clear positive trends.

5. Discussion

Volcanism in the Central Anatolia Volcanic Province started during the middle Miocene with the production of a few calc-alkaline basaltic andesite lavas, followed by abundant and widespread ignimbrite sheets varying in composition from dacite to rhyolite (e.g., Batum, 1978; Besang et al., 1977; Lepetit et al., 2014; Pasquaré, 1968; Piper et al., 2013; Temel et al., 1998). All large Cappadocia volcanoes continued their activity through the late Miocene and Pliocene, producing alternate lava flows and pyroclastic rocks with a high-K calc-alkaline petrological affinity (e.g., Alici Şen et al., 2004; Aydar et al., 2012; Aydar and Gourgaud, 1998; Aydin, 2008; Deniel et al., 1998; Gençalioğlu-Kuşcu and Geneli, 2010; Kürkçüoğlu et al., 1998, 2001; Notsu et al., 1995).

5.1. The Central Anatolia Volcanic Province Na-alkaline rocks

No Neogene Na-alkaline rocks have been found in the Central Anatolia Volcanic Province. The first Na-alkaline rocks formed during late monogenetic activity in the Karapınar, Eğrikuyu, South Hasan Dağ, Karataş, Kutören and Kızılırmak volcanic fields; in many cases these were emplaced after the calc-alkaline volcanic rocks, although in a few

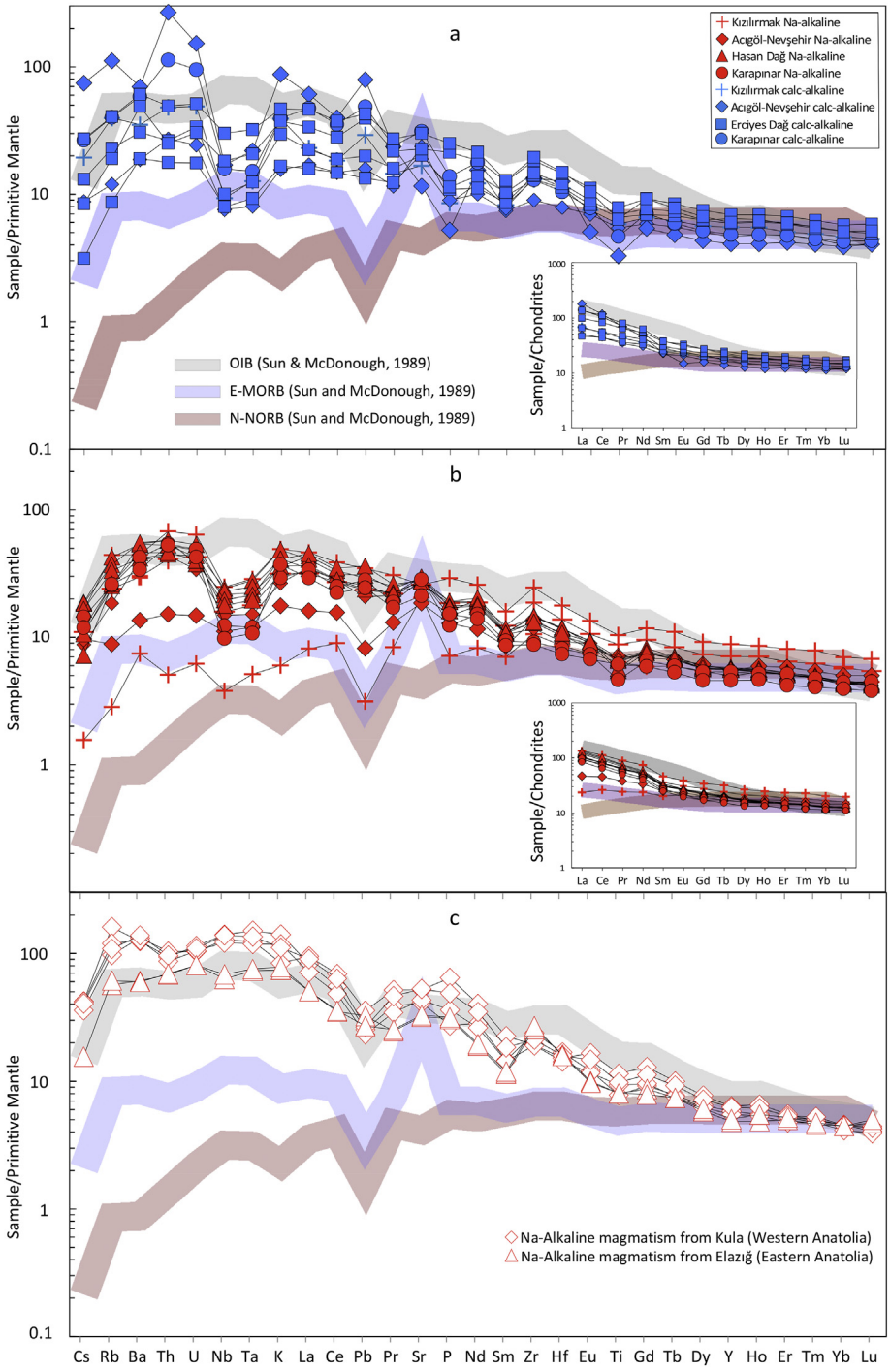

Fig. 5. Primitive mantle-normalized diagrams for the studied calc-alkaline (a) and Na-alkaline (b) samples; c) primitive mantle-normalized diagrams for Na-alkaline rocks from Western (Kula) and Eastern (Elazığ) Anatolia. Insets show CI-chondrite normalized REE diagrams for the studied rocks. Primitive mantle and CI-chondrite normalization factors, as well as OIB, *E*-MORB and N-MORB values, from Sun and McDonough (1989).

cases the Na-alkaline and calc-alkaline rocks are coeval (Supplementary Tables 1 and 3). Available age determinations on the studied samples indicate a Middle-Late Pleistocene (0.654–0.018 Ma; Aydin et al., 2014; Bigazzi et al., 1993; Ercan et al., 1990), Early-Late Pleistocene (0.78–0.47 Ma; Ercan et al., 1992, 1994; Reid et al., 2017) and Pliocene-Middle Pleistocene (3.6–0.15 Ma; Ercan et al., 1994; Innocenti et al., 1975; Notsu et al., 1995) for activity at the Acıgöl-Nevşehir, Hasan Dağ and Erciyes Dağ clusters, respectively.

These Na-alkaline volcanic rocks are mildly alkaline, with small amounts of normative *nepheline* (0–2.7 mol%) and no modal feldspathoids. Previous studies ascribe the occurrence of Na-alkaline volcanic rocks in the final monogenetic phases of activity in Cappadocia to a transitional affinity between the alkaline and tholeiitic end members (e.g. Aydin et al., 2014; Deniel et al., 1998; Gençalioğlu-Kuşcu, 2011; Gençalioğlu-Kuşcu and Geneli, 2010; Kürkçüoğlu et al., 2004). The Na-alkaline basalts of the Central Anatolia Volcanic Province are quite peculiar. In the primitive mantle-normalized multi-elemental diagrams, Na-alkaline magmas worldwide have a typical OIB-HiMu signature characterised by positive HFSE (e.g., Nb and Ta) anomalies (Hofmann, 1997), whereas subduction-related products

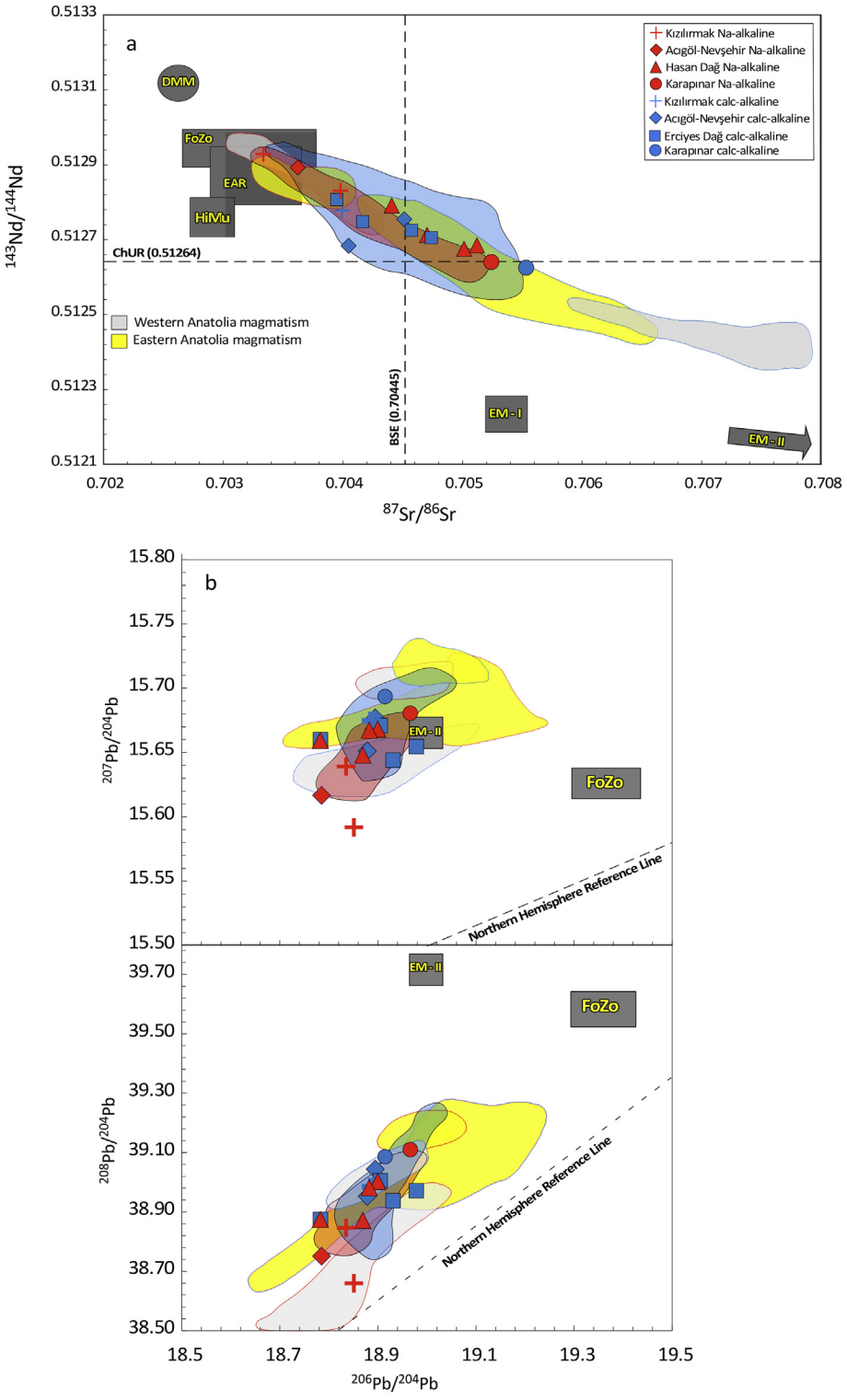

Fig. 6. a) $^{143}Nd/^{144}Nd$ vs. $^{87}Sr/^{86}Sr$ isotopic ratios for the studied samples. BSE = Bulk Silicate Earth. ChUR = Chondritic Uniform Reservoir; b) $^{207}Pb/^{204}Pb$ vs. $^{206}Pb/^{204}Pb$ and $^{208}Pb/^{204}Pb$ vs. $^{206}Pb/^{204}Pb$ diagrams. Dashed line indicates the Northern Hemisphere Reference Line (NHRL; Hart, 1984). Rectangles represent the mantle end-members from Zindler and Hart (1996); Cebriá and Wilson (1995) and Workman and Hart (2005); DMM = Depleted MORB Mantle; EAR = European Asthenospheric Reservoir; FoZo = Focal Zone; HiMu = High μ, where μ = $^{238}U/^{204}Pb$; EMI = Enriched Mantle I and EMII = Enriched Mantle II. Grey area: Western Anatolia Neogene magmatism; yellow area: Eastern Anatolian Neogene volcanic activity. Blue and red borders around the grey and yellow fields represent calc-alkaline and Na-alkaline magmatic activity, respectively. Data from Agostini et al. (2005, 2007); Aldanmaz et al. (2000, 2006); Arger et al. (2000); Buket and Temel (1998); Di Giuseppe et al. (2017); Innocenti et al. (2005). Light red and light blue areas as in Fig. 3.

exhibit marked LILE enrichments with respects to HFSE (e.g., Pearce, 1983). In contrast, in the Central Anatolia Volcanic Province, both groups of rocks exhibit marked LILE and LREE enrichments with respect to HFSE, associated with negative Ta and Nb anomalies, which could be attributed to the acquisition of a subduction-related signature during their genesis. In terms of trace element distribution and isotopes, the Cappadocia Na-alkaline rocks therefore also differ significantly from the typical OIB-like Na-alkaline volcanic rocks cropping out in the surrounding areas, e.g. in Western and Eastern Anatolia (Fig. 4 and 5).

The contemporaneous occurrence of Na-alkaline and calc-alkaline volcanic rocks in recent monogenetic activity at Cappadocia strongly suggests the contemporaneous activation of a mantle source of magmas. However, both the Sr-Nd-Pb isotopes and the trace element distribution of Cappadocia alkali basalts indicate that there are no pure within-plate alkaline (i.e., OIB-like) lavas in Cappadocia. In the next paragraph, we will investigate whether the absence of such products may be ascribed to magma contamination during evolution or to primitive source features.

5.2. Fractional crystallisation and crustal assimilation

Both the Na-alkaline and the calc-alkaline volcanic rocks follow differentiation trends to different extents (Fig. 4, Supplementary Figs. 1–2). Na-alkaline samples show a narrower range of silica and ferromagnesian element contents than calc-alkaline ones. Calc-alkaline rocks range from relatively primitive to strongly differentiated members (Mg# = 71–21 calc-alkaline), whereas Na-alkaline rocks show a narrower differentiation trend (Mg# = 72–51). In both series, the first step in differentiation is the fractionation of a Si-poor mafic assemblage such as olivine, clinopyroxene and Fe—Ti oxides. Full trace element variations against SiO_2 are reported in Supplementary Fig. 2. As shown in Fig. 5, most considerations on trace element variations during evolution come from the literature data. For trace element and radiogenic isotope analyses, all of our samples but one has $SiO_2 < 55$ wt%, because this study mainly aimed to investigate the characteristics of the source magma and not the effects of differentiation. The simultaneous decrease in major oxides such as Fe_2O_3, MgO, TiO_2 and CaO, as well as the negative trend in compatible elements V and Sc with increasing silica (Supplementary Figs. 1 and 2), indicate that the liquid lines of descent were controlled by fractional crystallisation of mainly clinopyroxene, whereas the negative correlation of Ni and Co with silica confirms the removal of olivine (Supplementary Fig. 2). In the intermediate members of the calc-alkaline series, the addition of plagioclase to the fractionating assemblage is clearly indicated by the decrease in Al_2O_3, Na_2O and Sr as silica increases; the low Eu/Eu* values (0.76–1.07) lend further support to the crystallisation of plagioclase. Plagioclase plays no apparent role in the differentiation of Na-alkaline rocks (Supplementary Table 2).

Variations in $^{87}Sr/^{86}Sr$ with silica and other major and trace elements (Fig. 4, Supplementary Figs. 1–2) suggest that open-system processes played a significant role in the differentiation of both series; a rough positive correlation, suggesting a significant amount of crustal contamination during magma evolution, can be seen for intermediate and evolved calc-alkaline samples (i.e. andesites to rhyolites, light blue field in Fig. 4c), whereas no $^{87}Sr/^{86}Sr$ vs. SiO_2 covariation is observed in Na-alkaline basalts and in less evolved calc-alkaline rocks. In addition, trace element ratios (e.g., Rb/Zr, Ba/La vs. Th/U; Fig. 7a) suggest that crustal contamination had a negligible effect, if any, on our poorly evolved samples. In contrast, the evolved calc-alkaline samples show a significant shift towards crustal values (Supplementary Fig. 2). In summary, we believe that crustal contamination can be ruled out in the limited differentiation path of Na-alkaline Cappadocia monogenetic

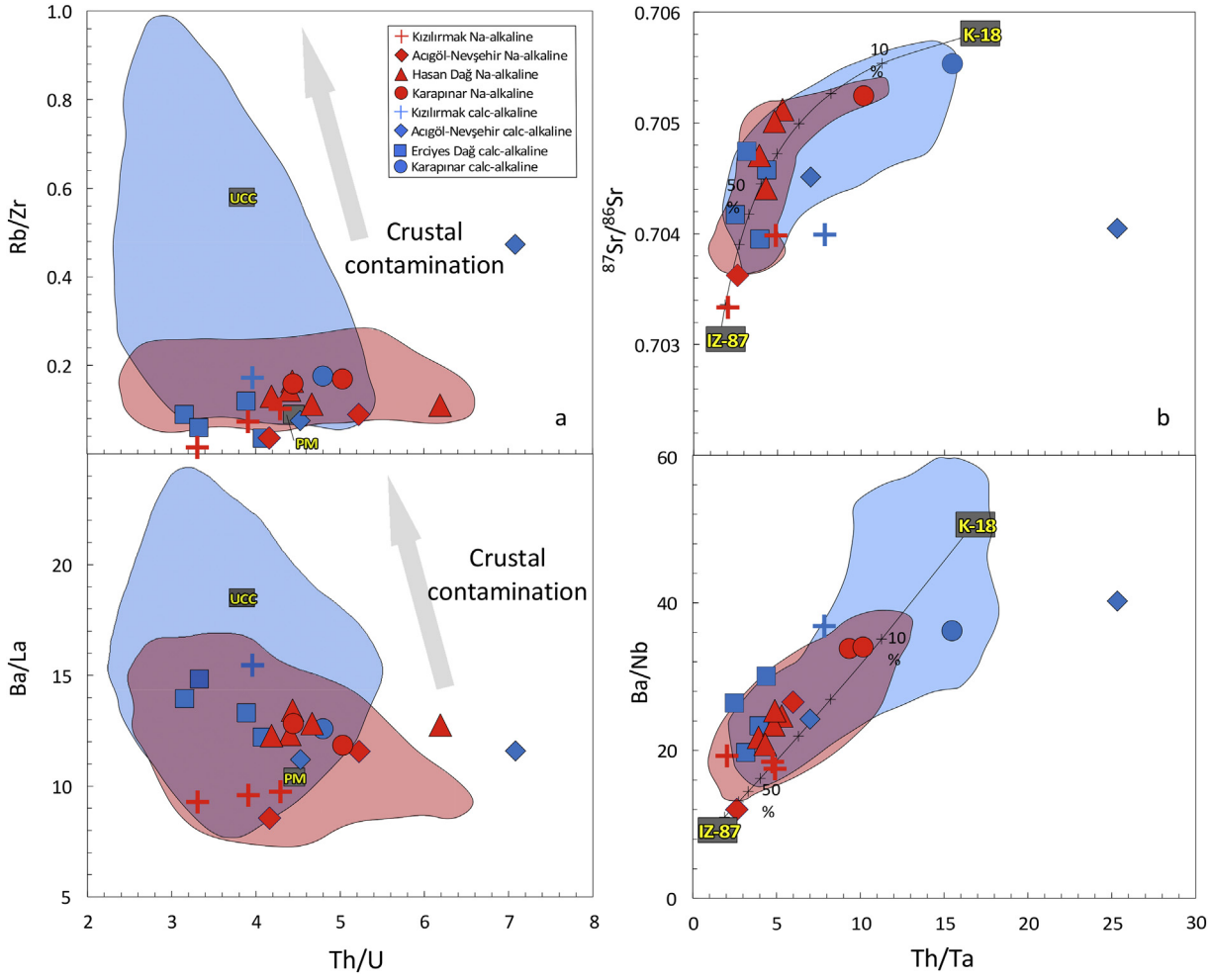

Fig. 7. a) Rb/Zr and Ba/La vs. Th/U diagrams. Primitive Mantle (PM) and Upper Continental Crust (UCC) values from Sun and McDonough (1989) and Taylor and McLennan (1985), respectively; b) $^{87}Sr/^{86}Sr$ and Ba/Nb vs. Th/Ta diagrams. Crosses along the mixing line represent the percentage of mixing for Na-alkaline and calc-alkaline end-members. Light red and light blue areas as in Fig. 3.

volcanism, as well as in the first stages of differentiation (basalts to basaltic andesites) of the calc-alkaline magmas. The LILE enrichments, the large Sr and Nd isotopic variations, and the HFSE and Ti depletions in the studied rocks must be considered mainly primary features inherited from mantle sources.

5.3. Insights into mantle source end-members

To better understand the characteristics of the source of Cappadocian magmatism, samples were plotted in the Ta/Yb vs. Th/Yb diagram (Fig. 8a), along with other volcanic products cropping out in Western and Eastern Anatolia. As reported in the previous paragraph, our dataset is not affected by AFC processes (high SiO_2-andesite sample CA 28 has been excluded from the following considerations). To minimise the effects of fractional crystallisation, as well as those of crustal contamination, we considered only samples from the literature with $SiO_2 < 60$ wt% and MgO > 3 wt% for calc-alkaline rocks and $SiO_2 < 52$ wt% and MgO > 4 wt% wt. for Na-alkaline samples. In Fig. 8a magmas derived from mid-plate or passive margins lie within or very close to the "Mantle Array" field, characterised by almost constant Th/Ta ratios. In contrast, rocks derived from sources modified by subduction-related metasomatism should retain Th enrichment relative to Ta and Yb (Pearce, 1982) and an upward shift, with higher Th/Yb values, for a given Ta/Yb ratio, e.g. pointing towards the Global Subducted Sediments (GloSS) field. As seen in Fig. 8a, samples from the Central Anatolia Volcanic Province, with both calc-alkaline and Na-alkaline affinity, plot well above the mantle array. Note that Na-alkaline rocks plot far from typical within-plate magmas with OIB-like signatures; their Th/Yb ratios are similar to those of Na-alkaline lavas from Kula (Western Anatolia) and Elazığ (Eastern Anatolia), but Ta/Yb ratios are at least one order of magnitude lower. This strongly suggests that a mantle source containing variable amounts of a subduction component was involved in the formation of all these magmas. Only two Na-alkaline basalts fall close to the mantle array: CA 57 and CA 27. These are the same samples characterised by FoZo-like Sr and Nd isotope values (Fig. 6), indicating that the role of a subduction-modified source was limited in the case of these two samples.

As previously reported, the studied rocks are characterised by variable degrees of enrichment in fluid-mobile elements such as Rb, Cs, Ba, Th and U. The enrichment in LILE relative to HFSE (e.g., Nb and Ta)

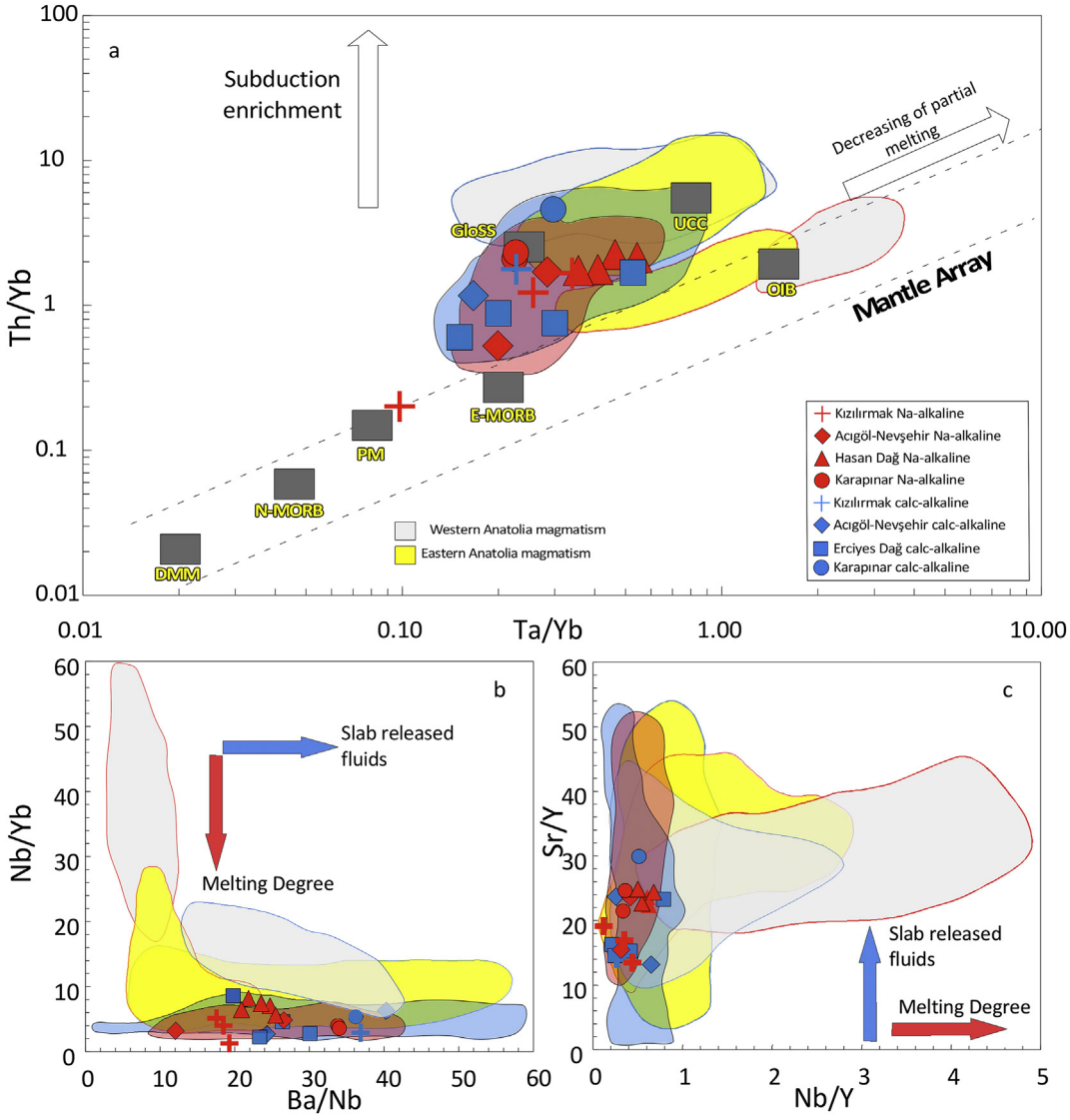

Fig. 8. a) Th/Yb vs. Ta/Yb diagram (after Pearce, 1983). DMM = Depleted MORB Mantle (values from Workman and Hart, 2005); N-MORB = Normal MORB, PM = Primitive Mantle, E-MORB = Enriched MORB and OIB = Oceanic Island Basalts (values from Sun and McDonough, 1989); UCC = Upper Continental Crust (values from Taylor and McLennan, 1985; GloSS = Global Subducted Oceanic Sediments (values from Plank and Langmuir, 1998). Fields as in Fig. 7; b) Ba/Nb vs. Nb/Yb and (c) Nb/Y vs. Sr/Y diagrams. Arrows represent increasing degrees of partial melting and fluid release by the slab. Coloured areas as in Fig. 6. Light red and light blue areas as in Fig. 3.

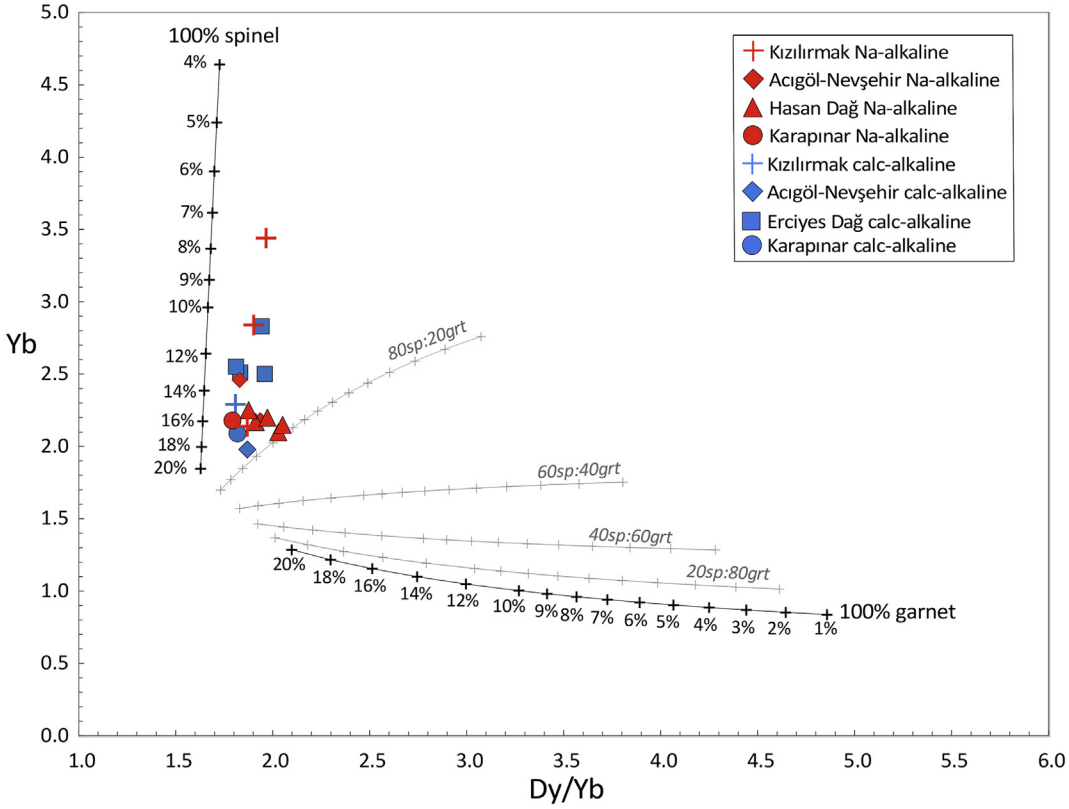

Fig. 9. Yb vs. Dy/Yb diagram for the studied rocks. Partial melting lines are drawn for garnet and spinel-bearing lherzolite sources, starting from a Primitive Mantle (PM; McDonough and Frey, 1989) material. Mineral and melt modes for spinel and garnet-lherzolite source are reported here: $Ol_{0.58(0.10)} + Opx_{0.27(0.27)} + Cpx_{0.12(0.50)} + Sp_{0.03(0.13)}$ (Kinzler, 1997) and $Ol_{0.60(0.05)} + Opx_{0.21(0.20)} + Cpx_{0.08(0.30)} + Gt_{0.12(0.45)}$ (Walter, 1998), respectively, in which the members in parentheses indicate the percentages of each mineral entering the liquid. Crosses along the melting trajectories represent the percentage of melting for spinel- and garnet-peridotite sources, respectively. Partition coefficients are from McKenzie and O'Nions (1991).

is usually attributed to subduction-related metasomatism, because of HFSE are mostly retained in the subducted slab during its progressive dehydration, whereas LILE and LREE migrate upward in slab-derived fluids or melts and then modify the overlying mantle wedge composition (e.g., Tatsumi, 1989). Trace element ratios (e.g., LILE/LREE, LILE/HFSE) such as Sr/Y vs. Nb/Y and Nb/Yb vs. Ba/Nb may be used to discriminate between aqueous fluids and silicate melts (Fig. 8b and c). Ba and Sr are elements that easily migrate in aqueous fluids, whereas Nb and Y are considered fluid-immobile. The marked increase in Ba/Nb and Sr/Y ratios and relatively constant Nb/Yb and Rb/Y ratios in our dataset suggest fluids as metasomatising agents rather than melts.

We modelled a non-modal batch melting process. As observed in the multi-element diagrams, the relatively flat HREE patterns of all suites should preclude garnet as a residual phase, suggesting a shallow asthenospheric mantle source for the magmas that gave rise to the Cappadocia calc-alkaline and Na-alkaline rocks. To strengthen this hypothesis, we modelled the partial melting of a spinel peridotite and a garnet peridotite mantle source (Fig. 9). The most mafic samples show two types of behaviour: Na-alkaline and calc-alkaline rocks from the Karapınar, Erciyes Dağ, Kızılırmak and Acıgöl-Nevşehir clusters plot along the evolution line for an almost garnet-free lherzolite source, whereas Hasan Dağ samples show a small shift towards garnet-bearing peridotites. According to this model, the degree of melting ranged from 7 to 16%, however, magma evolution process may lead to some overestimate thus these results have to be considered as maximum values.

5.4. Magma interaction: mixing process

Petrographic observation of volcanic samples revealed disequilibrium textures, such as poikolitic textures with opaque inclusions in feldspar phenocrysts. In addition, sieved, patchy and corroded textures in plagioclase coexisting with rounded and embayed clinopyroxene suggest magma mixing. This process has already been considered to play a major role in the formation of rocks from the Erciyes Dağ composite volcano (e.g., Kürkçüoğlu et al., 2004) and the Acıgöl-Nevşehir cluster, although in the latter district only a few studies have been carried out around the Acıgöl rhyolitic fields (Siebel et al., 2011).

The possible interaction between two different mantle domains beneath the Central Anatolia Volcanic Province is also suggested by:

1) the complete lack of volcanic products showing the true OIB-HiMu signature of an extensional regime, contrary to what has been observed in both Western (e.g., Agostini et al., 2005, 2010b; Innocenti et al., 2005) and Eastern Anatolia (e.g., Di Giuseppe et al., 2017);
2) the contemporaneous emplacement of calc-alkaline and Na-alkaline products during the Pleistocene and the coexistence of *q-normative*, *ol-hy-normative* and *ne-normative* rocks within the same volcanic cluster, as revealed by previous studies on recent magmatism in this region (e.g., Gençalioğlu-Kuşcu, 2011);
3) the similarities in radiogenic isotope compositions, as well as the similar LILE and HFSE distributions on mantle-normalized diagrams for calc-alkaline and Na-alkaline rocks.

Based on these observations, we modelled a mixing process using a primitive intraplate HiMu-OIB-like sample (IZ 87 from Kula; Innocenti et al., 2005) and a calc-alkaline subduction-related basaltic andesite (K-18 from Karapınar cluster; Notsu et al., 1995) as end members. Model results are shown in $^{87}Sr/^{86}Sr$ and Ba/Nb versus Th/Ta diagrams (Fig. 7b). In these diagrams, all the studied rocks fit with the mixing trend, testifying to the interaction between two different magmas: a) a calc-alkaline, SiO_2-oversaturated magma sourced in a shallower mantle with a clear contribution from a subduction component (i.e., the

mantle wedge); b) a Na-alkaline, OIB-like magma from a source not modified by subduction, such as the sub-slab asthenosphere. In this view, the lack of true OIB-like Na-alkaline within-plate igneous rocks in the Central Anatolia Volcanic Province may be explained by mixing of these two components. The variable degree of mixing between OIB-like and calc-alkaline magmas can explain the entire range of Na-alkaline Cappadocia rocks with subduction-related geochemical signatures. The results of mass balance calculations for the mixing model were reported in a multi-element variation diagram (Fig. 10). The addition of 13 wt% of the OIB-like end-member (sample IZ 87, Kula, Innocenti et al., 2005) to a calc-alkaline basalt (sample K-18; Notsu et al., 1995) is enough to produce an *hy + ol* normative melt, whereas ≥30 wt% of the same OIB-like end member would generate a *ne + ol* normative melt. The Nb—Ta positive anomaly, a distinctive feature of intraplate magmas, appears only after adding 86 wt% of the OIB-like end member. This means that each magma resulting from the addition of between 13 wt% and 86 wt% of an OIB-like end member will be a hybrid magma with Na-alkaline character, when considering major elements, and arc-like trace elements, when looking at spider diagrams. Among the Cappadocia Na-alkaline volcanic rocks, the composition of CA 57 is the one closest to the OIB-like end member; this, the youngest sample in our dataset (96 ± 13 ka, Koçyiğit and Doğan, 2016), is a transitional alkaline-tholeiitic basalt with an *E*-MORB-like pattern and a weak negative Nb and Ta anomaly.

6. Geodynamic scenario for central Anatolian volcanism

The geodynamic framework of the eastern Mediterranean region was controlled by the convergence of the African and Arabian plates with the Anatolide-Tauride blocks and the Eurasian Plate during the late Mesozoic and early Cenozoic (e.g., Dewey et al., 1986). This convergence culminated with the Arabia-Eurasia collision along the Bitlis-Zagros suture zone during the middle Miocene (e.g. Dewey et al., 1986; Faccenna et al., 2006;) and the subduction of the African Plate beneath the Eurasian Plate along the Aegean and Cyprus trenches starting in the early Miocene (e.g., Agostini et al., 2010a and references therein). Convergence was responsible for: a) deformation of the Anatolian block, resulting in a shortened and thickened continental crust in central and eastern Anatolia and the onset of intense magmatic activity (e.g. Şengör et al., 2003); b) the westward movement of Anatolia as an independent E-W-oriented microplate starting in the middle Miocene along the North Anatolian Fault (NAF; Şengör et al., 2005) and in the late Miocene-Pliocene along the East Anatolian Fault (EAF; e.g. Bozkurt, 2001). As result of this deformation, extensive magmatic activity occurred throughout western, central and eastern Anatolia, where both subduction-related calc-alkaline and Na-alkaline intraplate-type rocks were emplaced. Interestingly, a temporal shift between an older (early-middle Miocene) calc-alkaline magmatism with a clear subduction imprint and younger (late Miocene-Holocene) Na-alkaline activity with OIB-HiMu signatures is usually observed in different sectors of Turkey, such as Thrace (Yılmaz and Polat, 1998), the Biga Peninsula (Aldanmaz et al., 2000; Yılmaz et al., 2001), the Uşak-Kula-Akhisar region (Innocenti et al., 2005) and the Urla-Karaburun peninsula (Agostini et al., 2010b) to the west, and in the Kangal Basin (Kürkçüoğlu et al., 2015), Yamadağ-Malatya (Arger et al., 2000; Önal et al., 2008) and Elazığ-Tunceli (Di Giuseppe et al., 2017) to the east. Older alkali basalts have only been reported north of the study area, in the Sivas Basin (age ≈ 16.5–13.1 Ma, Maloney, 2014 and Platzman et al., 1998) and in the Galatia Province (between 20 and 17 Ma and 12–9 Ma; Keller et al., 1992, Wilson et al., 1997).

In Central Anatolia, in contrast, there is no observed temporal shift from calc-alkaline volcanism to Na-alkaline magmatism: the age of calc-alkaline magmatism is constrained between the late Miocene and the Pleistocene, and contemporaneous calc-alkaline and Na-alkaline monogenetic activity occurred only during the last phase, from the late Pliocene to the Pleistocene (e.g., Gençalioğlu-Kuşcu and Geneli, 2010). Pioneering studies have suggested that volcanic activity in the Central Anatolia Volcanic Province was related to active subduction along the Cyprus arc (Innocenti et al., 1975; Pasquaré, 1968; Temel et al., 1998) or by an ancient paleosubduction of this arc (e.g., Reilinger et al., 1997). However, the geochemical characteristics, the similar age of emplacement of both calc-alkaline and Na-alkaline products and

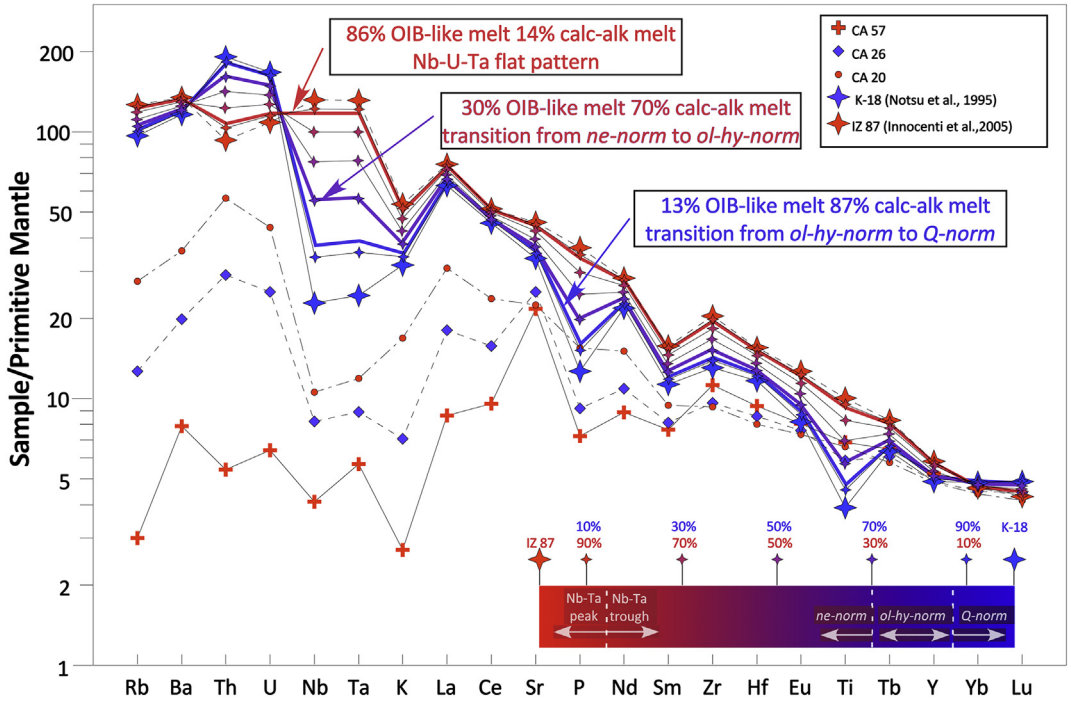

Fig. 10. Spider diagram depicting incompatible trace element patterns resulting from mixing between an OIB-type tephrite and a calc-alkaline basalt (see text for details). OIB-type end member in red, calc-alkaline end member in blue; variable degrees of mixing are indicated in purple. Transition points between Nb—Ta positive to negative anomalies, as well as from *Q-norm* to *ol-hy-norm* and from *ol-hy norm* to *ne-norm* are shown.

the geological evidences of a strike-slip to extensional tectonic setting, do not support the occurrence of typical arc-type volcanic activity. Alternatively, other authors (e.g., Kürkçüoğlu et al., 2004 and references therein) have pointed out that volcanism in the region was linked to decompression melting in response to extension in an intra-continental tectonic setting, suggesting either the presence of a heterogeneous mantle source or varying contributions by crustal materials. Deniel et al. (1998) and later Ilbeyli et al. (2004) and Alici Şen et al. (2004) proposed the presence of an enriched mantle source showing traces of an ancient subduction component. Similarly, Güçtekin and Köprübaşi (2009) and Gençalioğlu-Kuşcu (2011) also endorse this hypothesis, suggesting that volcanic activity in central Anatolia was in relation to the partial melting of a metasomatised subcontinental lithospheric mantle, followed by magma ascent facilitated by a transtensional tectonic regime. However, the relatively low $^{87}Sr/^{86}Sr$ and high $^{143}Nd/^{144}Nd$ of the calc-alkaline basaltic samples suggest a sublithospheric origin for these magmas (i.e. mantle wedge).

In this geodynamic context, the Cyprus slab plays an important but uncertain role in the tectonic development of the area (Reid et al., 2017). Biryol et al. (2011) claim that the slab beneath central Anatolia is fragmented and located at depths >200 km, suggesting that the location of the Cyprus slab is too deep to be the direct cause of recent monogenetic volcanism in the Central Anatolia Volcanic Province. Furthermore, central Anatolia is characterised by a high plateau-like topography (e.g. Şengör and Yılmaz, 1981), and recent studies evidenced that it is characterised by lithospheric thinning (e.g., McNab et al., 2018; Schildgen et al., 2014), slow seismic velocities beneath the upper mantle (e.g., Gans et al., 2009; Govers and Fichtner, 2016) and high heat flow (e.g., Uluocak et al., 2016). In addition, according to Öğretmen et al. (2018), most of the uplift took place in the last 450 ka (i.e. ≈1600 m on a total of ≈2000 m). Some authors (e.g. Abgarmi et al., 2017) infer that these features are linked to slab break-off and subsequent rebound. The occurrence of a high plateau and crustal thinning, coupled with the emplacement of Na-alkaline products may indicate the presence of uprising and a hot sub-lithospheric mantle, which was responsible for monogenetic volcanic activity. Many authors have reported the contribution of an asthenospheric mantle source with a clear subduction-related geochemical and isotopic signature to polygenetic and monogenetic activity in Cappadocia (e.g. Aydin et al., 2014; Gençalioğlu-Kuşcu and Geneli, 2010; Reid et al., 2017). Although the role and behaviour of the Cyprus slab in relation to volcanic activity in Cappadocia is still debated, the above-mentioned geophysical studies agree with the presence of a dominantly sublithospheric mantle source for recent volcanism in the Central Anatolia Volcanic Province, such that involvement of the Cyprus slab should be taken into account.

As mentioned earlier, Cappadocia volcanic activity is closely linked to the tectonic evolution of the area, with both monogenetic and polygenetic centres largely located along, or close to, the main strike-slip faults (Tuz Gölü, Ecemiş and Salanda fault systems) and surrounding depressions. The formation of deep transtensional systems favoured the ascent of the sublithospheric mantle. In this context, fault systems both generated areas of weakness in which magmas formed through decompression melting and acted as pathways through which magmas were channelled to the surface.

In this geodynamic scenario, the geochemical features of Central Anatolia volcanic activity show certain peculiarities: a) the Na-alkaline basalts are quite different from the typical intraplate-like OIB-HiMU lavas found throughout Anatolia because they show LILE/HFSE enrichments typical of calc-alkaline products; b) calc-alkaline and Na-alkaline rocks are characterised by very similar isotopic compositions, whereas other Na-alkaline Anatolian basalts (e.g. Biga, Kula, Elazığ) have markedly lower Sr and Pb isotopic compositions and higher $^{143}Nd/^{144}Nd$ ratios with respect to calc-alkaline products; c) the two rock series have similar emplacement ages; d) all the studied rocks show disequilibrium textures, suggesting interaction/mixing between two chemically and isotopically different mantle sources.

In summary, there are no true OIB-type magmas in Central Anatolia Volcanic Province, and Na-alkaline lavas are hybrid magmas resulting from mixing between melts originated in a pristine sublithospheric mantle source and calc-alkaline melts originated in a subduction-modified mantle domain. In the last 0.5 Ma Cappadocia has been characterised by two types of monogenetic products: hybrid OIB-type alkali basalts and calk-alkaline rocks. In addition, intense Pleistocene to Holocene calc-alkaline activity occurred in the main edifices of the two big composite volcanoes of Cappadocia, namely Hasan Dağ (Aydar and Gourgaud, 1998) and Erciyes Dağ (Şen et al., 2003). This magmatism is hard to reconcile with the occurrence of slab break-off and upwelling of a pristine asthenosphere that completely replaced the former subduction-modified mantle wedge. In this case, calc-alkaline activity would be absent (or residual) and abundant OIB-type

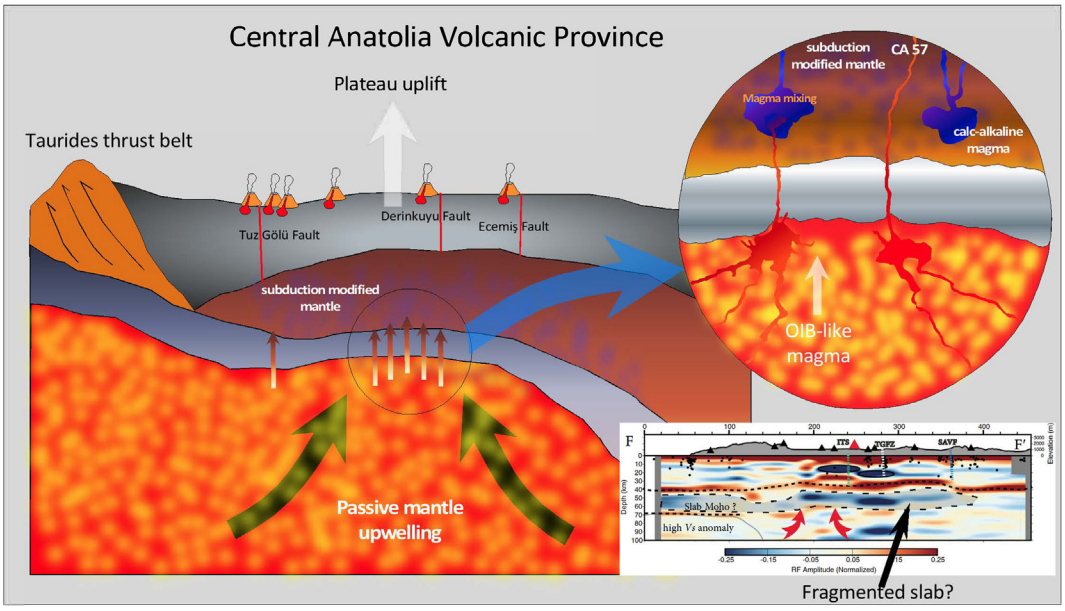

Fig. 11. Schematic illustration (not to scale) showing the geodynamic setting of the Central Anatolia Volcanic Province and (inset) the mantle sources of magmas.

magmas would reach the surface after little or no interaction with a modified mantle wedge or crustal lithologies. The Fig. 8 of Abgarmi et al. (2017) shows no evidence of slab break-off or slab steepening, but a sub-horizontal slab is present close to the trench, and some blue anomalies are present at depths of 50–70 km beneath the Cappadocian Volcanic Zone (Fig. 11, inset). These anomalies may represent the occurrence of a fragmented subhorizontal slab.

Fig. 11 shows a schematic model of possible interaction processes able to explain the peculiarity of Cappadocian Pliocene to Recent volcanic products. The ascent of the sublithospheric mantle and the products of subsequent decompression melting interacted and mixed with a mantle source previously metasomatised by subduction-released fluids, leading to the formation of spurious Na-alkaline magmas, the petrographic features and major element chemistry of which are quite similar to those of intraplate OIB-HiMu. However, these Na-alkaline basalts retain significant enrichments in fluid-mobile incompatible elements, as well as in radiogenic Sr and non-radiogenic Nd, with isotopic compositions typical of subduction-related products. Partial melting also affected some subduction-modified mantle domains, without any interaction with deeper Na-alkaline melts; as a result, pure OIB-types are lacking, but pure calc-alkaline products may be present. Note that the latter were not generated by typical arc volcanism, i.e. subduction-zone fluids metasomatizing the overlying mantle wedge and triggering its partial melting. Here, the metasomatizing event occurred mostly during active subduction, which lasted until the middle Miocene (e.g., Temel et al., 1998), whereas the mechanism responsible for calc-alkaline magma formation was mostly decompression melting linked to the Miocene to Recent strike-slip tectonic regime. As summarised in Fig. 11, hybrid Na-alkaline and calc-alkaline magmas formed contemporaneously in the region. The absence of clear within-plate alkaline magmas in the studied area might be re-conducted to the fact that the subducting slab, at this stage of geodynamic evolution of the Central Anatolia region, lacks of a fully opened plate window within the subducting slab, which would allow a continuous and abundant flux of sub-slab mantle within the mantle wedge. As a corollary, the limited occurrence of a torn, fragmented slab allowed the passage of limited volume of deep OIB-HiMu type material, which contaminated with shallower arc-related magmas during uprise to surface.

7. Conclusions

Research aimed to understand the nature of Neogene-Quaternary monogenetic activity in the Central Anatolia Volcanic Province, focusing on the Karapınar, Hasan Dağ, Acıgöl-Nevşehir, Kızılırmak and Erciyes Dağ clusters. A thorough geochemical, petrological, isotopical and geochronological study allowed us to distinguish two groups of rocks with different geochemical affinity but very similar age of emplacement:

(a) Calc-alkaline products, varying in composition from basalts to rhyolites, were emplaced during the late Pliocene (monogenetic activity of the Koç Dağ stage, within the Erciyes Dağ volcanic field) and throughout the Pleistocene; these rocks retain the typical chemical imprint of arc-related volcanism, that is geochemical and isotopic characteristics indicating that these magmas were sourced in a mantle wedge modified by slab fluids. These features include, for instance, marked LILE/HFSE enrichments, relatively high $^{87}Sr/^{86}Sr$ and low $^{143}Nd/^{144}Nd$.

(b) Na-alkaline basaltic to mugearitic rocks characterised by SiO_2 undersaturation and quite small major element variations formed in the Early Pleistocene to Late Pleistocene. These samples are characterised variable degrees of LILE enrichment and HFSE depletion, with variable but evident negative Nb-Ta-Ti troughs in the spider diagrams (Fig. 5). Their isotopic compositions are also very similar to those of calc-alkaline samples. The absence of true OIB-intraplate type magmas and the occurrence of such hybrid Na-alkali melts has been ascribed to mixing between subslab OIB-like magmas and magmas derived from the overlying subduction-modified mantle wedge. The sample with the weakest subduction signature is a very young basalt from the Kızılırmak cluster showing a typical *E*-MORB signature (CA 57, Fig. 11).

The geochemical characteristics of the studied rocks indicate that fractional crystallisation plus a certain amount of crustal assimilation were important in determining the evolution of these rock suites; however, the main differences depicted above are found in the less evolved magmas and are thus ascribed to source features.

In summary, geochemical and isotopic results, combined with regional geological data, suggest that mixing involved magmas from two different mantle domains: a) a shallow mantle with a clear subduction imprint (supra-slab mantle wedge) and b) a deeper sub-slab mantle not modified by any subduction component. The contemporaneous activation of two distinct mantle sources is a peculiar characteristic of Central Anatolia volcanism: the post-collisional transtensional tectonic regime favoured magma genesis via decompression melting and magma ascent through the well-developed fault system. Subduction is no longer active in the area, so that in the case of calc-alkaline magmas, contrary to what is observed in common arc lavas, the event that produced mantle wedge metasomatism (Oligocene-middle Miocene subduction) differs from that responsible for magma genesis (middle Miocene-Recent decompression melting).

Acknowledgements

The authors thank Z. Pecskay (MTA-Atomki, Debrecen, Hungary) and M. D'Orazio (DST-University of Pisa, Italy) for K—Ar ages and ICP-MS data, respectively, A. Rielli and T. Di Rocco for constructive criticism and discussion. A professional proofreading service reviewed the English style and grammar of the manuscript. Financial support was provided by IGG-CNR-P0000514 funds with S. Agostini as P.I., and by PRIN-2015 (grant # 20158A9CBM) with S. Conticelli as P.I. The final manuscript was greatly improved through thoughtful and constructive comments by the editor-in-chief, Andrew Kerr, and official peer-reviews by M. Cemal Göncüoğlu and anonymous.

Appendix A. Supplementary data

Supplementary data to this article can be found online at https://doi.org/10.1016/j.lithos.2018.07.018.

References

Abgarmi, B., Delph, J.R., Ozacar, A.A., Beck, S.L., Zandt, G., Sandvol, E., Turkelli, N., Biryol, C.B., 2017. Structure of the crust and African slab beneath the central Anatolian plateau from receiver functions: new insights on isostatic compensation and slab dynamics. Geosphere 13, 1774–1787.

Agostini, S., Doglioni, C., Innocenti, F., Manetti, P., Savaşçin, M.Y., Tonarini, S., 2005. Tertiary high-Mg volcanic rocks from Western Anatolia and their geodynamic significance for the evolution of the Aegean area. In: Fytikas, M., Vougioukalakis, G.E. (Eds.), The South Aegean Volcanic Arc Development in Volcanology 7. Elsevier, Amsterdam, pp. 345–362.

Agostini, S., Doglioni, C., Innocenti, F., Manetti, P., Tonarini, S., Savaşçın, M.Y., 2007. The transition from orogenic to intraplate Neogene magmatism in Western Anatolia and Aegean area. In: Beccaluva, L., Bianchini, G., Wilson, M. (Eds.), Cenozoic Volcanism in the Mediterranean Area. Geological Society of American, Special Paper vol. 418, pp. 1–15.

Agostini, S., Doglioni, C., Innocenti, F., Manetti, P., Tonarini, S., 2010a. On the geodynamics of the Aegean rift. Tectonophysics 488, 7–21.

Agostini, S., Tokçaer, M., Savaşçın, M.Y., 2010b. The transition volcanic rocks from Foça-Karaburun and Ayvalik-Lesvos grabens (western Anatolia) and their petrogenetic-geodynamic significance. Turk. J. Earth Sci. 19, 157–184.

Agostini, S., Manetti, P., Lustrino, M., Di Giuseppe, P., Savaşçın, M.Y., 2016. Central and Eastern Anatolia Volcanism. In: Agostini, S., Manetti, P., Lustrino, M. (Eds.), The Contribution of Italian Scientists to the Geology of the Turkey. Acta Vulcanologica vols. 26-27, pp. 37–50.

Agostini, S., Savaşçin, M.Y., Di Giuseppe, P., Di Stefano, F., Karaoğlu, Ö., Lustrino, M., Manetti, P., Ersoy, Y., Kürüm, S., Öztufekçi, A.Ö., 2018. Petrology and Stratigraphy of Neogene Volcanism In Elazığ- Tunceli Area (Eastern Anatolia Turkey) (submitted).
Aldanmaz, E., Pearce, J.A., Thirlwall, M.F., Mitchell, J.G., 2000. Petrogenetic evolution of late Cenozoic, post-collision volcanism in western Anatolia, Turkey. J. Volcanol. Geotherm. Res. 102, 67–95.
Aldanmaz, E., Köprübaşi, N., Gürer, Ö.F., Kaymakçı, N., Gourgaud, A., 2006. Geochemical constraints on the Cenozoic, OIB –type alkaline volcanic rocks of NW Turkey: implications for mantle sources and melting processes. Lithos 86, 50–76.
Alici Şen, P., Temel, A., Gourgaud, A., 2004. Petrogenetic modelling of quaternary post-collisional volcanism: a case study of central and eastern Anatolia. Geol. Mag. 141, 81–98.
Arculus, R.J., 2003. Use and abuse of the terms Calcaline and Calcalkalic. J. Petrol. 44, 929–935.
Arculus, R.J., Powell, R., 1986. Source component mixing in the regions of arc magma generation. J. Geophys. Res. 91, 5913–5926.
Arger, J., Mitchell, J., Westaway, R.W.C., 2000. Neogene and Quaternary volcanism of southeastern Turkey. In: Bozkurt, E., Winchester, J.A., Piper, J.D.A. (Eds.), Tectonics and Magmatism in Turkey and the Surrounding Area. vol. 173. Geological Society, London, pp. 459–487 Special Publication.
Avanzinelli, R., Lustrino, M., Mattei, M., Melluso, L., Conticelli, S., 2009. Potassic and ultrapotassic magmatism in the circum-Tyrrhenian region: the role of sediment recycling at destructive plate margin. Lithos 113, 213–227.
Avanzinelli, R., Prytulak, J., Skora, S., Heumann, A., Koetsier, G., Elliott, T., 2012. Combined 238U-230Th and 235U-231Pa constraints on the transport of slab-derived material beneath the Mariana Islands. Geochim. Cosmochim. Acta 95, 308–328.
Aydar, E., Gourgaud, A., 1998. The geology of mount Hasan stratovolcano, Central Anatolia, Turkey. J. Volcanol. Geotherm. Res. 85, 129–152.
Aydar, E., Schmitt, A.K., Çubukçu, H.E., Akin, L., Ersoy, O., Sen, E., Duncan, R.A., Atici, G., 2012. Correlation of ignimbrites in the central Anatolian volcanic province using zircon and plagioclase ages and zircon compositions. J. Volcanol. Geotherm. Res. 213-214, 83–97.
Aydar, E., Çubukçu, H.E., Sen, E., Akin, L., 2013. Central Anatolian plateau: incision and paleoaltimetry recorded from volcanic rocks. Turk. J. Earth Sci. 22, 739–746.
Aydin, F., 2008. Contrasting complexities in the evolution of calcalkaline and alkaline melts of the Niğde volcanic rocks, Turkey: textural, mineral chemical and geochemical evidence. Eur. J. Mineral. 20, 101–118.
Aydin, F., Schmitt, A.K., Siebel, W., Sönmez, M., Ersoy, Y., Lermi, A., Dirik, K., Duncan, R., 2014. Quaternary bimodal volcanism in the Niğde volcanic complex (Cappadocia, Central Anatolia, Turkey): age, petrogenesis and geodynamic implications. Contrib. Mineral. Petrol. 168, 1078.
Batum, I., 1978. Geology and petrography of Acıgöl and Göllüdağ volcanics at SW of Nevşehir, Central Anatolia, Turkey. Yerbilimleri 4, 50–69.
Besang, C., Eckhardt, F.J., Harre, W., Kreuzer, H., Muller, P., 1977. Radiometrische Altersbestimmungen an neogenen Eruptivgesteinen der Türkei. Jahrb. Geol. Bundesanst. 25, 3–36.
Bigazzi, G., Yeğingil, Z., Ercan, T., Oddone, M., Özdogan, M., 1993. Fission track dating obsidian in central and northern Anatolia. Bull. Volcanol. 55, 588–595.
Biryol, C.B., Beck, S.L., Zandt, G., Ozacar, A.A., 2011. Segmented African lithosphere beneath the Anatolian region inferred from teleseismic P-wave tomography. Geophys. J. Int. 184, 1037–1057.
Bonin, B., 2004. Do coeval mafic and felsic magmas in post-collisional to within plate regimes necessarily imply two contrasting, mantle and crustal, sources? A review. Lithos 78, 1–24.
Bozkurt, E., 2001. Neotectonics of Turkey- a synthesis. Geodin. Acta 14, 3–30.
Buket, E., Temel, A., 1998. Major-element, trace-element, and Sr-Nd isotopic geochemistry and genesis of Varto (Muş) volcanic rocks, eastern Turkey. J. Volcanol. Geotherm. Res. 85, 405–422.
Cebriá, J.M., Wilson, M., 1995. Cenozoic mafic magmatism in western/Central Europe; a common European asthenosphere reservoir. Terra Nova, Abstract Supplement. vol. 7, p. 162.
Conticelli, S., Manetti, P., Peccerillo, A., Santo, A., 1986. Caratteri petrologici delle vulcaniti potassiche italiane: considerazioni genetiche e geodinamiche. Mem. Soc. Geol. Ital. 35, 775–783.
Conticelli, S., Guarnieri, L., Farinelli, A., Mattei, M., Avanzinelli, R., Bianchini, G., Boari, E., Tommasini, S., Tiepolo, M., Prelević, D., Venturelli, G., 2009. Trace elements and Sr-Nd-Pb isotopes of K-rich, shoshonitic, and calc-alkaline magmatism of the western Mediterranean region: genesis of ultrapotassic to calc-alkaline magmatic associations in a post-collisional geodynamic setting. Lithos 107, 68–92.
Conticelli, S., Avanzinelli, R., Marchionni, S., Tommasini, S., Melluso, L., 2011. Sr-Nd-Pb isotopes from the Radicofani Volcano, Central Italy: constraints on heterogeneities in a veined mantle responsible for the shift from ultrapotassic shoshonite to basaltic andesite magmas in a post-collisional setting. Miner. Petrol. 103, 123–148.
Conticelli, S., Avanzinelli, R., Poli, G.E., Braschi, E., Giordano, G., 2013. Shift from lamproite-like to leucititic rocks: Sr–Nd–Pb isotope data from the Monte Cimino volcanic complex vs. the Vico stratovolcano, Central Italy. Chem. Geol. 353, 246–266.
Conticelli, S., Avanzinelli, R., Ammannati, E., Casalini, M., 2015. The role of carbon from recycled sediments in the origin of ultrapotassic igneous rocks in the Central Mediterranean. Lithos 232, 174–196.
Deniel, C., Aydar, E., Gourgaud, A., 1998. The Hasan Dağı stratovolcano (Central Anatolia, Turkey): evolution from calc-alkaline to alkaline magmatism in a collisional zone. J. Volcanol. Geotherm. Res. 87, 275–302.
Dewey, J.F., Hempton, M.R., Kidd, W.S.F., Şaroğlu, F., Şengör, A.M.C., 1986. Shortening of continental lithosphere: the neotectonics of Eastern Anatolia-a young collision zone. In: Coward, M.P., Ries, A.C. (Eds.), Collision Zone Tectonics. vol. 19. Geological Society, London, pp. 3–36 Special Publications.
Dhont, D., Chorowicz, J., Yürür, T., Froger, J.L., Köse, O., Gündogdu, N., 1998. Emplacement of volcanic vents and geodynamics of Central Anatolia, Turkey. J. Volcanol. Geotherm. Res. 85, 33–54.
Di Giuseppe, P., Agostini, S., Lustrino, M., Karaoğlu, Ö., Savaşçın, M.Y., Manetti, P., Ersoy, Y., 2017. Compression to strike-slip tectonics shift as revealed by Miocene-Pleistocene volcanism west of the Karlıova triple junction (East Anatolia). J. Petrol. 58 (10), 2055–2087.
Dirik, K., Göncüoğlu, M.C., 1996. Neotectonic characteristics of Central Anatolia. Int. Geol. Rev. 38, 807–817.
Dirik, K., Göncüoğlu, M.C., Kozlu, H., 1999. Stratigraphy and pre-Miocene tectonic evolution of the southwestern part of the Sivas Basin, Central Anatolia. Geol. J. 34, 303–319.
Doğan, U., 2011. Climate-controlled river terrace formation in the Kızılırmak Valley, Cappadocian section, Turkey: inferred from Ar-Ar dating of quaternary basalts and terraces stratigraphy. Geomorphology 120, 66–81.
Dogan-Kulahci, G.D., -2016. Chronological, Magmatological and Geochemical Study of Post-Collisional Basaltic Volcanism in Central Anatolia and Its Spatiotemporal Evolution. PhD Thesis. Univ. Blaise Pascal, Clermont Ferrand (France).
Dogan-Kulahci, G.D., Guillou, H., Gourgaud, A., Deniel, C., Temel, A., Varol, E., 2016. New K-Ar Ages of Post-Collisional Quaternary Basaltic Volcanism in the Central Anatolian Volcanic Province, Turkey. Goldschimidt Abstracts, p. 689.
Dogan-Kulachı, G.D., Temel, A., Gourgaud, A., Varol, E., Guillou, H., Deniel, C., 2018. Contemporaneous alkaline and calc-alkaline series in Central Anatolia (Turkey): Spatio-temporal evolution of a post-collisional quaternary basaltic volcanism. J. Volcanol. Geotherm. Res. 356, 56–74.
Doglioni, C., Agostini, S., Crespi, M., Innocenti, F., Manetti, P., Riguzzi, F., Savaşçın, M.Y., 2002. On the extension in western Anatolia and the Aegean Sea. J. Virtual Explor. 8, 1–17.
D'Orazio, M., 1995. Trace element determination in igneous rocks by ICP-MS: results on ten international reference samples. Period. Miner. 64, 315–328.
Druitt, T.H., Brenchley, P.J., Gökten, Y.E., Francaviglia, V., 1995. Late quaternary rhyolitic eruptions from Acıgöl complex, Central Turkey. J. Geol. Soc. Lond. 152, 655–667.
Duggen, S., Hoernle, K., Van Den Bogaard, P., Garbe-Schönberg, D., 2005. Post-collisional transition from subduction-to intraplate-type magmatism in the westernmost Mediterranean: evidence for continental-edge delamination of subcontinental lithosphere. J. Petrol. 46, 1155–1201.
Elliott, T.R., Plank, T., Zindler, A., White, W., Bourdon, B., 1997. Element transport from slab to volcanic front at the Mariana arc. J. Geophys. Res. 102, 14991–15019.
Ercan, T., Fujitani, T., Matsuda, J.I., Tokel, S., Notsu, K., Ui, T., Can, B., Selvi, Y., Yildirim, T., Fişekçi, A., Ölmez, M., Akbaşlı, A., 1990. The origin and evolution of the Cenozoic volcanism of Hasandağı-Karakadağ area, Central Anatolia (in Turkish). Bull. Geomorphol. 18, 39–54.
Ercan, T., Tokel, S., Matsuda, J.I., Ul, T., Notsu, K., Fujitani, T., 1992. New geochemical, isotopic and radiometric data of the quaternary volcanism of Hasandağı-Karacadağ (Central Anatolia). TJ. Bull. 7, 8–21 (in Turkish with English abstract).
Ercan, T., Tokel, S., Matsuda, J., Ul, T., Notsu, K., Fujitani, T., 1994. Erciyes Dağı (Orta Anadolu) Pliyo-Kuvaterner volkanizmasina ilşkin yeni jeokimyasal, izotopik, radyometrik veriler ve jeotermal enerji açısından önemi. Türkiye 6. Enerji Kongresi Bildiriler Kitabi 208–222.
Faccenna, C., Bellier, O., Martinod, J., Piromallo, C., Regard, V., 2006. Slab detachment beneath eastern Anatolia: a possible cause for the formation of the north Anatolian fault. Earth Planet. Sci. Lett. 242, 85–97.
Gans, C.R., Beck, S.L., Zandt, G., Biryol, C.B., Ozacar, A.A., 2009. Detecting the limit of slab break-off in Central Turkey: new high resolution Pn tomography results. Geophys. J. Int. 179, 1566–1572.
Gasperini, D., Blichert-Toft, J., Bosch, D., Del Moro, A., Macera, P., Albarède, F., 2002. Upwelling of deep mantle material through a plate window: evidence from the geochemistry of Italian basaltic Volcanics. J. Geophys. Res. 107, 23–67.
Gençalioğlu-Kuşcu, G., 2011. Geochemical characterization of a quaternary monogenetic volcano in Erciyes volcanic complex: Cora maar (central Anatolian Volcanic Province, Turkey). Int. J. Earth Sci. 100, 1967–1985.
Gençalioğlu-Kuşcu, G., Geneli, F., 2010. Review of post-collisional volcanism in the central Anatolian Volcanic Province (Turkey), with special reference to the Tepekoy volcanic complex. Int. J. Earth Sci. 99, 593–621.
Göncüoglu, M.C., Toprak, V., 1992. Neogene and quaternary volcanism of Central Anatolia: a volcanostructural evaluation. Bull. Sect. Volcanol. 26, 1–6.
Govers, R., Fichtner, A., 2016. Signature of slab fragmentation beneath Anatolia from full-waveform tomography. Earth Planet. Sci. Lett. 450, 10–19.
Güçtekin, A., Köprübaşi, N., 2009. Geochemical characteristics of mafic and intermediate volcanic rocks from the Hasandağ and Erciyes volcanoes (Central Anatolia, Turkey). Turk. J. Earth Sci. 18, 1–27.
Hart, S.R., 1984. A large-scale isotope anomaly in the southern hemisphere mantle. Nature 309, 753–757.
Hawkesworth, C.J., Herft, J.M., McDermott, F., Ellam, R.M., 1991. Destructive margin magmatism and the contributions from the mantle wedge and subducted crust. Aust. J. Earth Sci. 38, 577–594.
Hawkesworth, C.J., Gallagher, K., Hergt, J.M., McDermott, F., 1993. Mantle and slab contributions in arc magmas. Annu. Rev. Earth Planet. Sci. 21, 175–204.
Hofmann, A.W., 1997. Mantle geochemistry: the message from oceanic volcanism. Nature 385, 219–229.
Ilbeyli, N., Pearce, J.A., Thirlwall, M.F., Mitchell, J.G., 2004. Petrogenesis of collision-related plutonics in Central Anatolia, Turkey. Lithos 72, 163–182.
Innocenti, F., Mazzuoli, G., Pasquaré, F., Radicati Di Brozolo, F., Villari, L., 1975. The Neogene calcalkaline volcanism of Central Anatolia: geochronological data on Kayseri-Niğde area. Geol. Mag. 112, 349–360.
Innocenti, F., Agostini, S., Di Vincenzo, G., Doglioni, C., Manetti, P., Savaşçin, M.Y., Tonarini, S., 2005. Neogene and quaternary volcanism in western Anatolia: magma sources and geodynamic evolution. Mar. Geol. 221, 397–421.

Irvine, T.N., Baragar, W.R.A., 1971. A guide to the chemical classification of the common volcanic rocks. Can. J. Earth Sci. 8, 523–548.

Jaffey, N., Robertson, A., Pringle, M., 2004. Latest Miocene and Pleistocene ages of faulting, determined by $^{40}Ar/^{39}Ar$ single-crystal dating of airfall tuff and silicic extrusives of the Erciyes Basin, Central Turkey: evidence for intraplate deformation related to the tectonic escape of Anatolia. Terra Nova 16, 45–53.

Karaoğlu, Ö., Selçuk, A.S., Gudmundsson, A., 2017. Tectonic controls on the Karlıova triple junction (Turkey): implications for tectonic inversion and the initiation of volcanism. Tectonophysics 694, 368–384.

Keller, J., 1974. Quaternary maar volcanism near Karapinar in Central Anatolia. Bull. Volcanol. 38, 378–396.

Keller, J., Jung, D., Eckhardt, J., Kreuzer, H., 1992. Radiometric ages and chemical characterization of he Galatean andesite massif, Pontus, Turkey. Acta Vulcanol. 2, 267–276.

Kinzler, R.J., 1997. Melting of mantle peridotite at pressure approaching the spinel to garnet transition: application to mid-ocean ridge basalt petrogenesis. J. Geophys. Res. 102 (B1), 853–874.

Koçyiğit, A., Doğan, U., 2016. Strike-slip neotectonic regime and related structures in the Cappadocia region: a case study in the Salanda basin, Central Anatolia, Turkey. Turk. J. Earth Sci. 25. https://doi.org/10.3906/yer-1512-9.

Kürkçüoğlu, B., Sen, E., Aydar, E., Gourgaud, A., Gündogdu, N., 1998. Geochemical approach to magmatic evolution of Mt. Erciyes stratovolcano Central Anatolia, Turkey. J. Volcanol. Geotherm. Res. 85, 473–494.

Kürkçüoğlu, B., Sen, E., Temel, A., Aydar, E., Gourgaud, A., 2001. Trace-element modelling and source constraints for tholeiitic and calc-alkaline basalts from a depleted astenospheric mantle source, Mt. Erciyes stratovolcano, Turkey. Int. Geol. Rev. 43, 502–522.

Kürkçüoğlu, B., Sen, E., Temel, A., Aydar, E., Gourgaud, A., 2004. Interaction of Asthenospheric and lithospheric mantle: the genesis of Calc-alkaline volcanism at Erciyes volcano, Central Anatolia, Turkey. Int. Geol. Rev. 46, 243–258.

Kürkçüoğlu, B., Pickard, M., Şen, P., Hanan, B.B., Sayit, K., Plummer, C., Sen, E., Yurur, T., Furman, T., 2015. Geochemistry of mafic lavas from Sivas, Turkey and the evolution of Anatolian lithosphere. Lithos 232, 229–241.

Le Maitre, R.W. (Ed.), 2002. Igneous Rocks. A Classification and Glossary of Terms. Cambridge University Press, Cambridge, p. 236.

Le Pennec, J.-L., Bourdier, J.L., Froger, J.L., Temel, A., Camus, G., Gourgaud, A., 1994. Neogene ignimbrites of the. Nevşehir plateau (Central Turkey): stratigraphy, distribution and source constraints. J. Volcanol. Geotherm. Res. 63, 59–87.

Le Pennec, J.-L., Temel, A., Froger, J.-L., Sen, S., Gourgaud, A., Bourdier, J.-L., 2005. Stratigraphy and age of the Cappadocia ignimbrites, Turkey: reconciling field constraints with paleontologic, radiochronologic, geochemical and paleomagnetic data. J. Volcanol. Geotherm. Res. 141, 45–64.

Le Pichon, X., Gaulier, J.M., 1988. The rotation of Arabia and the Levant fault system. Tectonophysics 153, 271–294.

Lepetit, P., Viereck, L., Piper, J.D.A., Sudo, M., Gürel, A., Çopuroğlu, I., Gruber, M., Mayer, B., Koch, M., Tatar, O., Gürsoy, H., 2014. $^{40}Ar/^{39}Ar$ dating of ignimbrites and plinian airfall layers from Cappadocia, Central Turkey: implications to chronostratigraphic and eastern Mediterranean palaeoenvironmental record. Chem. Erde 74, 471–488.

Lustrino, M., Wilson, M., 2007. The circum-Mediterranean anorogenic Cenozoic igneous province. Earth Sci. Rev. 81, 1–65.

Lustrino, M., Duggen, S., Rosenberg, C.L., 2011. The central-western Mediterranean: anomalous igneous activity in an anomalous collisional tectonic setting. Earth Sci. Rev. 104, 1–40.

Maloney, P.M., 2014. Melting Conditions of Basaltic Volcanism From Collision to Escape in the Central Anatolian Volcanic Province, Central Turkey. Master thesis. Northern Arizona University, p. 158.

McDonough, W.F., Frey, F.A., 1989. Rare earth elements in upper mantle rocks. Rev. Mineral. Geochem. 21 (1), 100–145.

McKenzie, D.P., O'Nions, R.K., 1991. Partial melt distributions from inversion of rare earth element concentrations. J. Petrol. 32, 1027–1091.

McKenzie, D.P., Davies, D., Molnar, P., 1970. Plate tectonics of the Red Sea and East Africa. Nature 226, 243–248.

McNab, F., Ball, P.W., Hoggard, M.J., White, N.J., 2018. Neogene uplift and magmatism of Anatolia: insights from drainage analysis and basaltic geochemistry. Geochem. Geophys. Geosyst. 19:175–213. https://doi.org/10.1002/2017GC007251.

Middlemost, E.A.K., 1975. The basalt clan. Earth-Sci. Rev. 11, 337–364.

Notsu, K., Fujitani, T., Ui, T., Matsuda, J., Ercan, T., 1995. Geochemical features of collision-related volcanic rocks in central and eastern Anatolia, Turkey. J. Volcanol. Geotherm. Res. 64, 171–192.

Öğretmen, N., Cipollari, P., Frezza, V., Faranda, C., Karanika, K., Gliozzi, E., Radeff, G., Cosentino, D., 2018. Evidence for 1.5 km of uplift of the central Anatolian Plateau's southern margin in the last 450 kyr and implications for its multiphased uplift history. Tectonics 37, 359–390.

Önal, A., Boztuğ, D., Arslan, M., Spell, T.L., Kürüm, S., 2008. Petrology and ^{40}Ar-^{39}Ar age of the bimodal Orduzu Volcanics (Malatya) from the western end of the eastern Anatolian Neogene volcanism, Turkey. Turk. J. Earth Sci. 17, 85–109.

Özsayin, E., Çiner, A., Rojay, B., Dirik, K., Melnick, D., Fernandez-Blanco, D., Bertotti, G., Schildgen, T.F., Garcin, Y., Strecker, M.R., Sudo, M., 2013. Plio-quaternary extensional tectonics of the central Anatolian plateau: a case study from Tuz Gölü Basin, Turkey. Turk. J. Earth Sci. 22, 1–24.

Pasquaré, G., 1968. Geology of the Cenozoic volcanic area of Central Anatolia, Turkey. Atti della Accademia Nazionale dei Lincei 9, 53–204.

Pasquaré, G., Poli, S., Vezzoli, L., Zanchi, A., 1988. Continental arc volcanism and tectonic setting in Central Anatolia, Turkey. Tectonophysics 146, 217–230.

Pearce, J.A., 1982. Trace element characteristics of lavas from destructive plate boundaries. In: Thorpe, R.S. (Ed.), Andesites. John Wiley & Sons, New York, pp. 525–548.

Pearce, J.A., 1983. Role of the sub-continental lithosphere in magma genesis at active continental margins. In: Hawkesworth, C.J., Norry, M.J. (Eds.), Continental Basalts and Mantle Xenoliths. Shiva Publishing Ltd, Nantwich, pp. 230–249.

Piper, J.D.A., Koçbulut, F., Gürsoy, H., Tatar, O., Viereck, L., Lepetit, P., Roberts, A.P., Akpınar, Z., 2013. Palaeomagnetism of the Cappadocian volcanic succession, Central Turkey: major ignimbrite emplacement during two short (Miocene) episodes and Neogene tectonics of the Anatolian collage. J. Volcanol. Geotherm. Res. 262, 47–67.

Plank, T., 2005. Constraints from thorium/lanthanum on sediment recycling at subduction zones and the evolution of the continents. J. Petrol. 46, 921–944.

Plank, T., Langmuir, C.H., 1998. The chemical composition of subducting sediment and its consequences for the crust and mantle. Chem. Geol. 145, 325–394.

Platzman, E.S., Tapirdamaz, C., Sanver, M., 1998. Neogene anticlockwise rotation of Central Anatolia (Turkey): preliminary palaeomagnetic and geochronological results. Tectonophysics 299, 175–189.

Prelević, D., Akal, C., Foley, S.F., Romer, R.L., Stracke, A., Den Bogaard, Van, 2012. Ultrapotassic mafic rocks as geochemical proxies for post-collisional dynamics of orogenic lithospheric mantle: the case of southwestern Anatolia, Turkey. J. Petrol. 53, 1019–1055.

Reid, M., Schleiffateth, W.K., Cosca, M.A., Delph, J.R., Blichert-Toft, J., Cooper, M.K., 2017. Shallow melting of MORB-like mantle under hot continental lithosphere, Central Anatolia. Geochem. Geophys. Geosyst. https://doi.org/10.1002/2016GC006772.

Reilinger, R.E., McClusky, S.C., Oral, M.B., 1997. Overview of the late Triassic-recent tectonic and palaeo-environmental development of the Mediterranean region. Terra Nova 7, 114–127.

Schildgen, T.F., Yıldırım, C., Cosentino, D., Strecker, M.R., 2014. Linking slab break-off, Hellenic trench retreat, and uplift of the central and eastern Anatolian plateaus. Earth Sci. Rev. 128, 147–168.

Şen, E., Kürkcüoğlu, B., Aydar, E., Gourgaud, A., Vincent, P.M., 2003. Volcanological evolution of mount Erciyes stratovolcano and origin of the Valibaba Tepe ignimbrite (Central Anatolia, Turkey). J. Volcanol. Geotherm. Res. 125, 225–246.

Şengör, A.M.C., Yılmaz, Y., 1981. Tethyan evolution of Turkey. A plate tectonic approach. Tectonophysics 75, 181–241.

Şengör, A.M.C., Özeren, S., Genç, T., Zor, E., 2003. East Anatolian high plateau as a mantle supported, northsouth shortened domal structure. Geophys. Res. Lett. 30:8045. https://doi.org/10.1029/2003GL017858.

Şengör, A.M.C., Tüysüz, O., İmren, C., Sakinç, M., Eyidoğan, H., Görür, N., Le Pichon, X., Ranging, C., 2005. The north Anatolian fault; a new look. Annu. Rev. Earth Planet. Sci. 33, 37–112.

Serri, G., Innocenti, F., Manetti, P., 2001. Magmatism from Mesozoic to Present: petrogenesis, time-space distribution and geodynamic implications. In: Vai, G.B., Martini, I.P. (Eds.), Anatomy of an Orogen: The Apennines and Adjacent Mediterranean Basins. Kluwer Academic Publishers, pp. 77–104.

Shaw, J.E., Baker, J.A., Menzies, M.A., Thirlwall, M.F., Ibrahim, K.M., 2003. Petrogenesis of the largest intraplate volcanic field on the Arabian plate (Jordan): a mixed lithosphere asthenosphere source activated by lithospheric extension. J. Petrol. 44, 1657–1679.

Siebel, W., Schmitt, A.K., Kiemele, E., Danišik, M., Aydin, F., 2011. Acigöl rhyolite field, Central Anatolia (part II): geochemical and isotopic (Sr-Nd-Pb, $\delta^{18}O$) constraints on volcanism involving two high-silica rhyolite suites. Contrib. Mineral. Petrol. 162, 1233–1247.

Smith, G.P., Weins, D.A., Fischer, K.M., Dorman, L.M., Webb, S.C., Hildebrand, J.A., 2001. A complex pattern of mantle flow in the Lau backarc. Science 292, 713–716.

Steiger, K.H., Jäger, E., 1977. Subcommission on geochronology: convention on the use of decay constantsin geo- and cosmochronology. Earth Planet. Sci. Lett. 36, 359–362.

Sun, S., McDonough, W.F., 1989. Chemical and isotopic systematics of oceanic basalts: implications for mantle composition and processes. In: Saunders, A.D., Norry, M.J. (Eds.), Magmatism in the Ocean Basins. vol. 42. Geological Society, London, pp. 313–345 Special Publications.

Tatsumi, Y., 1989. Migration of fluid phases and genesis of basalt magmas in subduction zones. J. Geophys. Res. 94, 4697–4707.

Taylor, S.R., McLennan, S.M., 1985. The Continental Crust; its Composition and Evolution; an Examination of the Geochemical Record Preserved in Sedimentary Rocks. Blackwell, Oxford, p. 312.

Taymaz, T., Eyidoğan, H., Jackson, J., 1991. Source parameters of large earthquakes in the east Anatolian fault zone (Turkey). Geophys. J. Int. 106, 537–550.

Temel, A., Gundoğdu, M.N., Gourgaud, A., Le Pennec, J.-L., 1998. Ignimbrites of Cappadocia (Central Anatolia, Turkey): petrology and geochemistry. J. Volcanol. Geotherm. Res. 85, 447–471.

Todt, W., Cliff, R.A., Hanser, A., Hofmann, A.W., 1993. Re-calibration of NBS lead standards using a 202Pb −205 Pb double spike. Terra Abstracts 5 (1), 396.

Toprak, V., 1998. Vent distribution and its relation to regional tectonics, Cappadocian Volcanics, Turkey. J. Volcanol. Geotherm. Res. 85, 55–67.

Toprak, V., Göncüoğlu, M.C., 1993. Tectonic control on the evolution of the Neogene-quaternary central Anatolian Volcanic Province, Turkey. Geol. J. 28, 357–369.

Turner, S., Hawkesworth, C., 1998. Using geochemistry to map mantle flow beneath the Lau Basin. Geology 26, 1019–1022.

Uluocak, E.Ş., Pysklywec, R., Göğüş, O.H., 2016. Present-day dynamic and residual topography in Central Anatolia. Geophys. J. Int. 206, 1515–1525.

Uslular, G., Gençalioğlu-Kuşcu, G., Arcasoy, A., 2015. Size-distribution of scoria cones within the Eğrikuyu monogenetic field (Central Anatolia, Turkey). J. Volcanol. Geotherm. Res. 301, 56–65.

Walter, M.J., 1998. Melting of garnet peridotite and the origin of komatiite and depleted lithosphere. J. Petrol. 39, 29–60.

Wilson, M., Tankut, A., Guleç, N., 1997. Tertiary volcanism of the Galatia Province, northwest Central Anatolia, Turkey. Lithos 42, 105–121.
Workman, R.K., Hart, S.R., 2005. Major and trace element composition of the depleted MORB mantle (DMM). Earth Planet. Sci. Lett. 231, 53–72.
Yılmaz, Y., Polat, A., 1998. Geology and evolution of the Thrace volcanism, Turkey. Acta Volcanol. 10 (2), 293–303.
Yılmaz, Y., Genç, Ş.C., Karacık, Z., Altunkaynak, Ş., 2001. Two contrasting magmatic associations of NW Anatolia and their tectonic significance. J. Geodyn. 31 (3), 243–271.
Zindler, A., Hart, S., 1996. Chemical geodynamics. Annu. Rev. Earth Planet. Sci. 14, 493–571.